6

Time-Resolved Laser Spectroscopy of Semiconductors - Physical Processes and Methods of Analysis

T. Brudevoll[1], A. K. Storebo[1], O. Skaaring[2], C. N. Kirkemo[3],
O. C. Norum[4], O. Olsen[4] and M. Breivik[5]
[1]*FFI (Norwegian Defence Research Establishment), Kjeller*
[2]*Kongsberg Defence and Areospace, Kjeller*
[3]*Department of Physics, University of Oslo, Oslo*
[4]*Department of Physics, Norwegian University of Science and Technology, Trondheim*
[5]*Department of Electronics and Telecommunications*
Norwegian University of Science and Technology, Trondheim
Norway

1. Introduction

Time-resolved laser spectroscopy has become an important method for extracting optical and transport parameters of semiconductors and semiconductor nanostructures. In many of the spectroscopic techniques using lasers the material is brought into a state far away from thermal equilibrium. Interpreting the non-equilibrium state of the material often constitutes a considerable challenge. Many different types of quasiparticles are involved, free electrons and different flavors of holes as well as excitons in many variants, all coupled to lattice modes or hybrid lattice/charge-carrier modes. Spin and magnetic systems are included among the cases considered important. A simplification that can be made under low-level laser irradiation using long pulses is to assume that carrier and lattice temperatures are equal with no excess sample heating. Once this 'isothermal' assumption is broken, sophisticated analysis tools must be used, even for seemingly simple problems and regardless of laser pulse length.

There is now a vast literature dealing with the results from time-resolved laser spectroscopy experiments. In particular, the book by Shah (Shah, 1999) covers the fundamentals of the subject. However, this field is in very rapid progress, and therefore the text will mainly emphasize later works. We describe new developments and survey the current state of the art regarding methods used for analyzing experiments, assuming some basic à priori knowledge of key experimental techniques. We shall do this survey by taking particular examples from the literature which in our opinion defines some of the main trends. By extracting the essence of selected papers and adding some of our own recent results, we hope to provide a useful guide for those interested in the subject of laser-matter interactions. Obviously, this type of interaction lies at the heart of many future technologies. Because of its central position, laser spectroscopy has become a mixture of old and new theoretical

tools, many of which takes years to learn and do well. Accordingly, any presentation of these tools runs a great risk of being bogged down with complicated mathematical relations and a time-consuming, heavy burden of pages. To avoid this, we restrict ourselves wherever possible to key ideas and relations actually needed for the experiments that we discuss, and present them in the context of their immediate use. Naturally, this comes at the expense of some loss of theoretical completeness, but in this way it quickly becomes clear what kind of theory is needed and how to continue with a narrow, well-targeted search for further background material.

2. Main spectroscopic techniques

Carrier dynamics in semiconductors can be explored by means of nonlinear laser spectroscopic techniques such as optical pump and probe spectroscopy, four-wave mixing, and transient gratings. In addition, time-resolved photoluminescence has been used to study hot-carrier relaxation and exciton formation. The main method used in time-resolved laser spectroscopy is the pump-probe technique. A strong pump pulse brings the material into a non-equilibrium state. Energetic excess charge carriers are generated by the pump pulse, and a weak probe pulse at specific delay times after the pump pulse instantly probes the state of the material. The delay of the probe beam provides the time resolution of the experiment.

Many different realizations exist. Development of new mid-infrared ultrafast laser sources makes photons with lower energies available, being well suited to probe intraband transitions. The response of free carriers and intra-exciton transitions can be studied with sub-picosecond temporal resolution. Mid-infrared probing of electron-hole (*e*-*h*) droplet formation in the direct gap semiconductor CuCl is a particularly striking example (Nagai et al. 2001). It is possible to extract information by utilizing either the reflected or the transmitted probe signal. On longer timescales the pump beam can give rise to luminescence from recombining excitons or electron-hole pairs. This luminescence can be analyzed, and e.g. the time evolution of the carrier temperature can be extracted. By using circularly polarized light instead of linearly polarized light, it is possible to induce imbalances in the spin (spin polarization) of the photoexcited carriers, producing, say, more spin up than spin down electrons. An accurate analysis of spin systems is possible by time-resolved two-photon photoemission, Faraday effect, and differential transmission spectroscopy (DTS). Also the prospect of controlling nuclear spins using optics is currently investigated (Makhonin et al., 2010). A particularly interesting case to study as semiconductor device dimensions shrink would be carrier dynamics and scattering occurring at material boundaries. Recent progress in experimental techniques suggests that five-wave mixing setups will provide access to such processes, (Voelkmann, 2004, Meier 2005).

Another important recent development is the introduction of combined ultrafast laser and terahertz THz methods, such as Terahertz time-domain spectroscopy (THz-TDS). Here an ultrafast laser is the pump, and the THz beam is the probe. To an even larger degree than mid-infrared lasers, a THz beam can probe the intraband properties of a semiconductor because the photon energy is much too low to generate band to band transitions. Unlike optical methods, THz-TDS enables the determination of the complex dielectric function (or optical conductivity) from which one can quantitatively evaluate the carrier density and the scattering time of the photoexcited carriers without resorting to the Kramers-Kronig relation. THz radiation can be generated in many ways, see (Blanchard et al., 2011) for an overview.

Furthermore, in semiconductors with medium or wide band gaps the excitonic effects are often significant, and here THz probing becomes very useful. A laser pump beam can create excitons, either directly by exciting an electron from the valence band into the 1*s* hydrogenic state of the exciton, or indirectly by exciting the electron from the valence band high into the conduction band. After a while, as the excess energy of the electron is dissipated by phonon scattering, it condenses into a hydrogenic-like state with a valence band hole, having a total energy less than the semiconductor band gap. The THz field can now directly probe the intraexciton transitions.
Finally, knowledge of the cooling dynamics in photoexcited *e-h* plasmas may also be of some interest in the study of low-temperature quantum-degenerate effects (Butov et al., 2002).

3. Laser pulselength regimes

3.1 General

In laser experiments involving band-to-band transitions, two types of carriers are generated, electrons and holes. In semiconductors electrons usually have much smaller effective masses than holes, and therefore electrons initially receive most of the laser energy. A simplified band structure for a direct gap semiconductor is shown in Fig. 1.

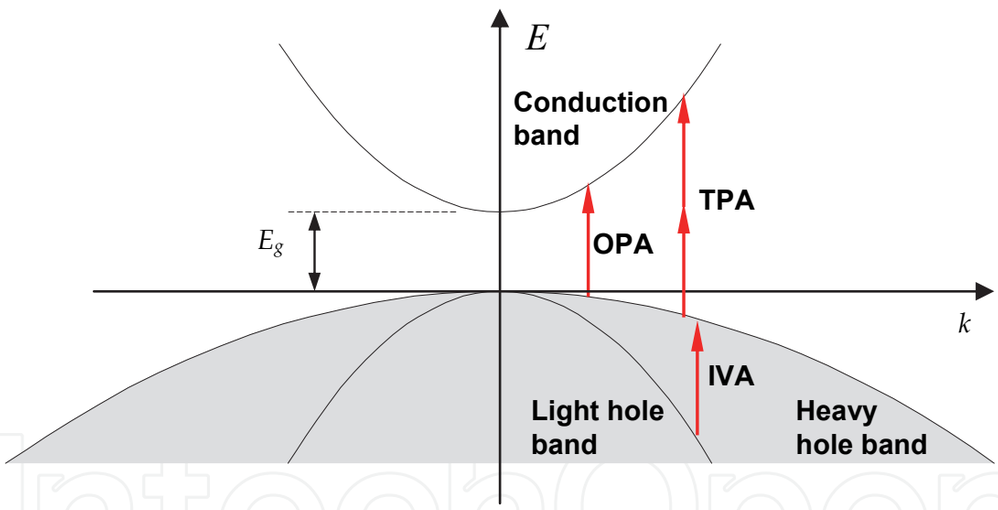

Fig. 1. Illustration of the band structure and important absorption processes in a direct gap semiconductor: OPA – one-photon absorption, TPA – two-photon absorption, IVA – inter-valence band absorption. In addition there will be absorption of radiation by free carriers, and there will be radiative or non-radiative recombination of electrons and holes. The shaded area indicates that the valence band is essentially fully occupied at thermal equilibrium, while the conduction band is empty. Below the heavy and light hole bands there is a split-off band, which in cases of strong spin-orbit splitting is separated from the former bands by a considerable energy gap (not shown).

Short pulses and short time delays between pump and probe sometimes help us to avoid the estimation of recombination effects and provide a very direct insight into carrier relaxation and hot phonon generation phenomena by isolating these processes from subsequent effects that occur on longer timescales. Energy transfer due to long, high fluence laser pulses on the

other hand, often increases the overall lattice temperature, but makes possible the investigation of many additional physical effects. In particular, if the photon energy of the incident radiation just exceeds the band gap, absorption can be highly non-linear and depend strongly on wavelength, radiation intensity, carrier temperatures, and lattice temperatures (Storebo et al., 2010).

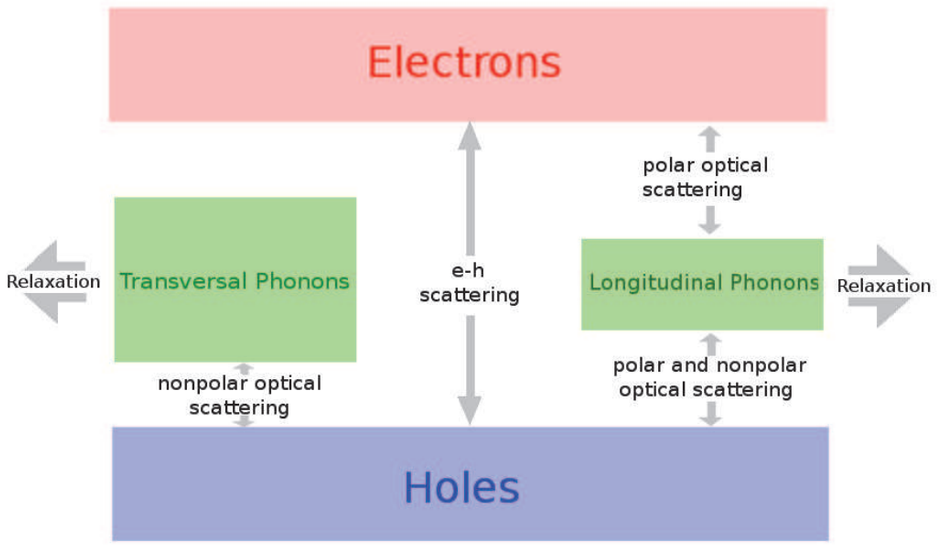

Fig. 2. Laser energy pathways between the different carrier ensembles. Electrons and holes initially pick up the laser energy. The ensembles are directly connected through electron-hole scattering, as well as indirectly through the longitudinal phonon distribution. The excess energy of the system can exit through both longitudinal and transversal phonons.

Laser energy pathways between the different carrier ensembles are illustrated in Fig. 2. We shall now make a tour through the different timescales of the laser experiments and discuss the physics-related issues as they arise.

3.2 Coherent ultrafast regime

In an ideally coherent regime the excitations of a laser irradiated quantum system would maintain a well-defined phase relation with the laser field. This coherence is rapidly destroyed by various scattering or collision processes, and therefore these influences can never be completely disregarded, but should rather be incorporated into the theory. A collision has a finite duration defined by the oscillation period of the energy quantum exchanged during the collision. In GaAs, the oscillation period of optical phonons is ~ 115 fs and the oscillation period of the electron plasma (plasmons are longitudinal collective carrier oscillations) is ~ 150 fs at a carrier density of $5 \cdot 10^{17} \mathrm{cm}^{-3}$. The interval between collisions can often be 100-200 fs. The dynamics of the coherent regime can be explored using differential transmission spectroscopy (DTS) (Shah, 1999) with laser pulses much shorter than the characteristic times given above, that is, on the order of 10 fs or shorter. Bulk materials, semiconductor microcavities, and nanostructures are investigated. Schemes for avoiding de-coherence is also an important aspect of future quantum information systems.

3.2.1 Semiconductor Bloch Equations (SBE)

Much of the early analysis on this subject matter has been carried out using the Semiconductor Bloch Equations (SBE), which we shall examine next. We note that SBE are most frequently used in situations where the optical properties are prominent, typically for excitations near the band gap, and for describing the dynamics of excitons and semiconductor lasers. If we treat the charge carriers by quantum mechanics and the radiation field classically, we arrive at the following standard equations for the polarization density, electron density, and hole density (Haug & Koch, 2009)

$$\begin{aligned}
\frac{\partial \mathrm{P}_{\boldsymbol{k}}}{\partial \mathrm{t}} &= -\mathrm{i}\left(\mathrm{e}_{\mathrm{e},\boldsymbol{k}} + \mathrm{e}_{\mathrm{h},\boldsymbol{k}}\right)\mathrm{P}_{\boldsymbol{k}} - \mathrm{i}\left(\mathrm{f}_{\mathrm{e},\boldsymbol{k}} + \mathrm{f}_{\mathrm{h},\boldsymbol{k}} - 1\right)\omega_{\mathrm{R},\boldsymbol{k}} + \left(\frac{\partial \mathrm{P}_{\boldsymbol{k}}}{\partial \mathrm{t}}\right)_{\mathrm{coll}} \\
\frac{\partial \mathrm{f}_{\mathrm{e},\boldsymbol{k}}}{\partial \mathrm{t}} &= -2\,\mathrm{Im}\left(\omega_{\mathrm{R},\boldsymbol{k}}\mathrm{P}_{\boldsymbol{k}}^{\,*}\right) + \left(\frac{\partial \mathrm{f}_{\mathrm{e},\boldsymbol{k}}}{\partial \mathrm{t}}\right)_{\mathrm{coll}} \\
\frac{\partial \mathrm{f}_{\mathrm{h},\boldsymbol{k}}}{\partial \mathrm{t}} &= -2\,\mathrm{Im}\left(\omega_{\mathrm{R},\boldsymbol{k}}\mathrm{P}_{\boldsymbol{k}}^{\,*}\right) + \left(\frac{\partial \mathrm{f}_{\mathrm{h},\boldsymbol{k}}}{\partial \mathrm{t}}\right)_{\mathrm{coll}}
\end{aligned} \tag{1}$$

We now proceed to explain the meaning of the various terms occurring in the above equations. In separating out the time variation of the polarization variables $\mathrm{P}_{\mathbf{k}}$ and the carrier occupation variables $\mathrm{f}_{i\boldsymbol{k}}$ (where $i = e,h$) due to collisions as we have done here it has been assumed that the non-collision terms correspond to the time-dependent Hartree-Fock approximation and that the collision terms are corrections to Hartree-Fock. This is reflected in the expressions for the single-particle energies $\mathrm{e}_{\mathrm{e},\mathbf{k}}$ and $\mathrm{e}_{\mathrm{h},\mathbf{k}}$ defined as

$$\hbar \mathrm{e}_{\mathrm{i},\boldsymbol{k}} = \hbar\varepsilon_{\mathrm{i},\boldsymbol{k}} + \mathrm{i}\sum_{\mathrm{exch,i}}(\boldsymbol{k}) = \hbar\varepsilon_{\mathrm{i},\boldsymbol{k}} - \sum_{\boldsymbol{q}} \mathrm{V}_{|\boldsymbol{k}-\boldsymbol{q}|}\mathrm{f}_{\mathrm{i},\boldsymbol{q}} \tag{2}$$

In band structure terminology the single particle energies in the Hartree-Fock approximation includes a part of the contribution from carrier-carrier interactions called exchange (Ashcroft & Mermin, 1976, Ch. 17). The strength of the carrier-carrier interactions are given by the parameter V_{q}. The exchange energy $\sum_{\mathrm{exch}}$ renormalizes the single particle energies $\hbar\varepsilon_{\mathrm{i,k}}$. If further interaction terms are included, this is called correlation (or collision) terms.

When an electron is excited from the valence band a hole is created. This electron and the corresponding hole create a microscopic polarization in the form of a dipole to which the incoming radiation field $\boldsymbol{E}$ couples. Propagation effects of the radiation field must explicitly be taken into account by simultaneously solving the wave equation, e.g. by a numerical scheme such as the Finite Difference Time-Domain method. Electrons and holes can either form excitons or free electron-hole pairs. The factor $-(\mathrm{f}_{\mathrm{e,k}} + \mathrm{f}_{\mathrm{h,k}} - 1) = \mathrm{f}_{\mathrm{v,k}} - \mathrm{f}_{\mathrm{c,k}}$ represents the population inversion at $\boldsymbol{k}$, that is, the difference between electron occupation of the valence band state $\boldsymbol{k}$ and electron occupation of the conduction band state $\boldsymbol{k}$. This factor influences the absorption spectrum of the material by state filling effects. The strength of the interband dipole coupling to the radiation field is given by the generalized Rabi frequency,

$$\omega_{\mathrm{R},\boldsymbol{k}} = \frac{1}{\hbar}\left[\boldsymbol{d}_{\mathrm{c,v}} \cdot \boldsymbol{E} + \sum_{\boldsymbol{q}\neq\boldsymbol{k}} \mathrm{V}_{|\boldsymbol{k}-\boldsymbol{q}|}\mathrm{P}_{\boldsymbol{q}}\right] \tag{3}$$

where $d_{c,v}$ is the transition dipole moment between initial and final states, obtained by a summation over the positions of the charge carriers i,

$$\boldsymbol{d} = e\left(\sum_i x_i, \sum_i y_i, \sum_i z_i\right) \tag{4}$$

and calculating the matrix element of the vector ***d***.

Remember that the Rabi frequency is a semiclassical concept representing the frequency of population oscillation between the levels of a resonantly illuminated two-level system. When the system is illuminated it will cyclically absorb photons and reemit them by stimulated emission. The Rabi frequency is a measure of the coupling strength between the electronic system and the radiation field. We see from the form of the equation for $\omega_{R,k}$ that the electron-hole system reacts to the combination of the applied field ***E***(t) and the polarization field of the generated electron-hole pairs. Absorption of radiation and generation of electrons and holes are described by the factor $-2\,\mathrm{Im}\left[\omega_{R,k} P_k^*\right]$.

At first glance, the equations for electron occupation and hole occupation appear very similar. If scattering is ignored, the rate of change in electron and hole populations are identical, and the two equations do not seem to mix different momentum states ***k***. But a closer look reveals that Coulomb terms in the generalized Rabi frequency and in the exchange energy in fact lead to such a coupling.

The original two-level SBE assume a scalar field and were not designed to account for the degrees of freedom connected with carrier spin or with the transversality of the exciting radiation. Spin is related to the concept of exchange, which we will encounter several times in the following sections. The charge carriers are fermions, and as such they must have antisymmetric wavefunctions under exchange of identical particles. Antisymmetry can either come from the spin or the spatial part of the wavefunction, and is responsible for how particles arrange themselves. This can be viewed as a kind of particle interaction, and including exchange is therefore vital in many cases. Exchange effects are a manifestation of the Pauli exclusion principle.

Spin and the transversality of the radiation field are somehow connected. Optical excitation with circular polarization generates spin-polarized carrier populations (optical spin alignment) and can be used to investigate spin dynamics. Research on spin-dependent phenomena in semiconductors is progressing in many different directions. Much of the emphasis within spintronic device research is related to long-lived electron-spin polarization and long-range transport properties. But outside the mainstream one still finds many interesting effects to be studied. For example, in materials lacking inversion symmetry, the resulting small splitting of degenerate single-particle electronic states is connected to the circular photogalvanic effect, CPGE (Ganichev, 2000, 2001). Spin relaxation times can be measured by noticing that the nonlinear absorption is different for linear and circular polarized excitation. (Ganichev, 2002).

In spin systems, not only the electrons are important. The hole spin may also be used to carry information. Holes play an important role for magnetic correlations in diluted magnetic semiconductors, as we shall see in a later section. From a fundamental point of view, holes in III–V semiconductors are a model system for spin relaxation with pronounced spin-orbit (SO) coupling. The SO coupling leads to a strong momentum dependent mixing

of spin and orbital-momentum eigenstates, so that scattering processes can change spin and orbital angular momentum. Although both electrons and holes are affected by this relaxation mechanism, it causes a much faster spin relaxation for the *p*-like holes than the *s*-like electrons, because the former experience the SO coupling directly, while the mainly *s*-like conduction band only achieves an orbital momentum by a weak coupling to remote bands with nonzero orbital momentum.

The mechanisms of spin relaxation for bulk and for semiconductor quantum wells are quite similar. The dominant ones for most semiconductor structures under investigation are the D'yakonov-Perel' (DP) mechanism, related to the spin-splitting of the single-particle states in systems lacking inversion symmetry, and the Bir-Aronov-Pikus (BAP) mechanism, caused by spin flip electron-hole exchange scattering processes. In addition, we have the phonon- or impurity-mediated spin flip Elliot-Yafet mechanism.

A detailed understanding of the processes contributing to spin relaxation on ultrashort timescales is impossible using simplified relaxation-time approximations. And we have seen that we must consider holes as well as electrons. Before we mention alternative approaches to include spin and the transversality of the radiation, it is useful first to take a look at the difficulties involved. It is important to remember that the field of spin dynamics is an aspect of carrier dynamics. Historically, numerical transport theory schemes used for the calculation of carrier dynamics did not resolve the spin of the charge carriers. But it is perfectly possible to incorporate spin into these schemes to analyze ultrafast spin-dependent optical experiments. Therefore we shall first take a short step back and consider spin from a traditional transport theory viewpoint.

In the transport theory approach, band structures are first calculated and used as input for the calculation of the momentum and time-dependent carrier distribution functions including the relevant interaction mechanisms.

By combining a realistic band structure with simulations of the evolving carrier distribution function, we can achieve a quantitative physical picture of the hole-spin dynamics, which in turn can be confirmed by optical experiments. A typical model system for such experiments is GaAs, having rather strong spin-orbit coupling. Krauss et al. (Krauss, 2008) obtained theoretical spin-relaxation times in quantitative agreement with measured hole-spin relaxation times, but it also turned out that a careful analysis of the experimental setup was necessary to achieve this agreement. They showed that different optical techniques for the measurement of hole-spin dynamics gave different results, in contrast to the case of the much simpler electron-spin dynamics. In particular, the relation between spin and band eigenstates (quasiparticle states) is not as simple as for electrons. Therefore different relaxation times for the quasiparticle polarization and the spin polarization have to be defined, and further related to the polarization extracted from differential transmission measurements. In electron dynamics, all these quantities coincide and can reveal the degree of spin polarization.

Extension of the SBE formalism in order to treat the dynamics of holes including the spin and polarization degrees of freedom can be found in e.g. (Rössler, 2003). Here a six band model is used for the heavy hole, light hole, and spin-orbit split off band, each of these three bands containing two spin degrees of freedom (Fig. 1). Undoubtedly, treating hole dynamics with the SBE is complicated. We only mention here a long standing issue regarding the polarization-dependent four wave mixing (FWM) quantum beats, which have been observed after simultaneous excitations of two optical transitions, i.e. heavy hole and light hole. The signal

magnitude and its beat phase depend on the polarization of the pump and probe with respect to each other, and this can in principle be analyzed with Bloch equations (SBE) in a six-band model. However, such a theory would predict identical FWM intensities for the two polarization configurations, with pump and probe having either parallel or perpendicular polarizations. Much work has been devoted to explain this phenomenon theoretically. One of the successful, but disputed (Wang al. 2006) candidates for explanation is the bi-exciton theory, which includes exciton-exciton interactions not included in standard SBE.

In the literature, we now find specific SBE formulations for quantum wells, wires, and dots (Kira et al., 1999, Haug & Koch, 2009, Feldtmann, 2009). We especially mention formulations for carbon nanotubes (Hirtschulz et al. 2008).

In carbon nanotubes (CNTs), many-body effects such as electron-electron and electron-phonon interactions play an important role, and excitons couple to vibronic modes. Much of the work on CNTs so far has dealt with the steady-state response of these excitations to cw fields. Frequency domain descriptions using Hubbard models (Ma & Yuan 1998, Lopez-Sancho et al. 2001) or *ab initio* density functional theory and the Bethe-Salpeter equation (Chang et al. 2004) have been developed. The Bethe-Salpeter equation is well suited for describing excitonic effects, but such calculations are linked to *ab initio* electronic structure methods and this combination can be extremely computer intensive. See e.g. (Christensen et al., 2011) for an update on the merits of such approaches. In contrast, Hirtschulz et al. describe a compact dynamical method for CNT properties which seems very useful for the study of ultrashort laser-induced nonlinear optical response. Many-body density matrix theory was combined with tight-binding band structure calculations of CNTs. It was shown that the derived carbon nanotube Bloch equations contained excitons as elementary optical excitations, both for low-level excitation as well as for optical nonlinearities and gain induced at higher excitations. They illustrated the temporal response to ultrashort pulses by calculating the time dependence of the electron density and the optical Stark effect.

3.2.2 Simplification by the use of excitonic bases

Several approaches have been developed to study the nonlinear optical response of semiconductors. Non-equilibrium Green's function and density matrix techniques are among the most common (Haug & Jauho, 1996, Haug & Koch, 2009, Mahan, 2007). Semiconductor Bloch equations (SBEs) are based on the density matrix, as are the dynamics controlled truncation (DCT) equations, which are an alternative to the Hartree-Fock treatment of the SBE mentioned above. Standard SBE have some drawbacks. Coulomb interaction between free electrons and holes require the Hartree-Fock procedure, which readily give the excitons but cannot describe exciton-exciton interactions. In addition, the solution of coupled SBE equations is a rather demanding numerical task.

In recent years it has become clear that using a different basis can greatly simplify this task for cases where excitonic effects dominate. Instead of using free electrons and holes as the starting point of the theory, one can use correlated pairs, i.e. excitons as basic operators. In ordinary SBE, the Coulomb interactions between carriers are cut by the HF method we saw above to get a closed, but numerically heavy set of equations. This truncation scheme leads to a spurious divergence in the carrier-carrier scattering rate, which must be fixed by a manual procedure. Higher-order Coulomb correlations cannot be incorporated unless other computationally intensive methods are chosen, such as the Bethe-Salpeter Equation or non-equilibrium Greens functions.

Excitons being composite bosons, do not have strict commutation rules. It becomes impossible to treat interactions between excitons through an effective exciton Hamiltonian $H_{ex} + U_{exex}$, where U_{exex} is the interaction potential between excitons regarded as elementary bosons. As a consequence, standard many-body techniques will not work, because they all depend on a perturbative expansion in the interaction potential U_{exex}.

By using exciton based SBE (Haug & Koch, 2009, Feldtmann, 2009) or other exciton based approaches (Combescot et al., 2003, Wang, 2009, Wang & Dignam, 2009), to study specific problems, we can achieve substantial simplifications. The method of Combescot et al. leads to an analytic expression for the polarization induced by the laser pulse, with the two sources for the polarization, Pauli blocking and Coulomb interaction becoming tracable troughout the calculation.

An excitonic basis requires a certain mapping (or pairing) of electrons to holes. This mapping of the electron-hole basis onto the excitonic basis is not one-to-one. For example, if we have two electrons and two holes in specific single-particle states, there are two different ways in which these electrons could be paired with the holes.

If we introduce a certain pairing scheme, this ambiguity may be resolved. Two such schemes will be described here. The first is to restrict an electron-hole pair to be in a given internal exciton state. In most cases it will be most profitable to choose the 1*s* state. We then allow the center-of-mass momentum $\mathbf{K}_{CM}$ of the pair to take any value, and call this choice the state-restricted exciton basis. The second approach is to pair electrons and holes that have opposite momenta, meaning that the resulting exciton will have $\mathbf{K}_{CM} = \mathbf{0}$ (remember that photons carry a very small momentum and will therefore create $\mathbf{K}_{CM} \sim \mathbf{0}$ excitons directly). Now these momentum-restricted excitons can have any internal state 1*s*,2*s*,2*p*, including continuum exciton states.

In order to find the best scheme for a given problem, we must consider their strengths and weaknesses. For example, a 1s state-restricted approach requires resonant optical excitation of 1*s* excitons and cannot account for THz-induced transitions between different internal excitonic states e.g., 1*s* to 2*p*. But the freedom in momentum allows us to study four-wave mixing and examine the time evolution of exciton momenta, including scattering of excitons to optically inactive excitonic states with nonzero $\mathbf{K}_{CM}$. The state-restricted scheme can also to a certain degree account for the formation of biexcitons.

The fixed-momentum approach cannot describe four-wave mixing and the formation of biexcitons. Interactions between excitons are limited by the restriction in momentum, and include only the exchange effect, which sometimes can be dominant. However, because it includes all internal states, it allows for excitation to states other than the 1s state, and can account for scattering of the optically active excitonic states into optically inactive excitonic states. Furthermore, Terahertz induced transitions between excitonic internal states can be modeled, as well as state-filling effects. In the coherent regime, most of the excitons still have $\mathbf{K}_{CM} = \mathbf{0}$ momentum. Including only $\mathbf{K}_{CM} = \mathbf{0}$ excitons is therefore not a serious limitation on short timescales.

A central problem with excitonic bases is how to deal with state-filling effects associated with the composite nature of excitons. State-filling results in non-bosonic carrier density-dependent commutation relation for the excitonic operators. At low carrier densities, state-filling is negligible and the excitons will obey boson commutation rules. At moderate excitation densities this is a reasonable approximation. Another alternative is to “bosonize”

the excitons, resulting in creation and annihilation operators following strict boson commutation rules. Bosonization schemes are still debated, with difficulties defining an effective Hamiltonian (Combescot et al., 2003).

On the other hand, it is sometimes possible to just accept and use the non-bosonic exciton creation and annihilation operators, and to explicitly take their exact density-dependent commutation relations into account, as explained in the paper by Wang & Dignam (Wang & Dignam, 2009). This can be done by first defining a set of quasi-boson states. These are electron-hole pair states consisting of the natural electron and hole single-particle eigenstates of the semiconductor structure, paired so that the total momentum $\mathbf{K}_{CM} = \mathbf{0}$. Based on quasi-boson commutation rules and a quasi-boson Hamiltonian. the dynamical equations for the quasi-boson operators are obtained. The true excitons are a superposition of quasi-boson states, and this superposition then defines the actual transformation between quasi-bosons and true excitons. Thus, dynamic equations for the true excitons finally appear by a transformation from the corresponding quasi-boson dynamic equations.

Wang & Dignam used a momentum-restricted $\mathbf{K}_{CM} = \mathbf{0}$ excitonic basis including state-filling and exchange to study the excitonic influence on the ultrafast nonlinear absorption in quantum wells. The optical pulse was resonant on the 1*s* exciton. They found that, the momentum-restriction notwithstanding, resonant excitation of the 1*s* exciton state at moderate carrier densities $\sim 1.3 \cdot 10^{10}\,\mathrm{cm}^{-2}$ could be described by further restricting the basis to 1*s* exciton states only. However, for higher carrier densities $\sim 5.0 \cdot 10^{10}\,\mathrm{cm}^{-2}$, the 1*s* peak was reduced and blueshifted and the band edge was redshifted. These effects on the absorption can only be described correctly if the coupling of the 1*s* states to both optically active and inactive higher exciton states is taken into account. Again, characteristic for the use of excitonic bases, it was possible to obtain analytical expressions for the density-dependent blueshift and bleaching of the 1*s* excitonic resonance for the case of moderate carrier densities.

To summarize, the approximations we have seen here are made possible by a close scrutiny of the excitation conditions, finding that only a small portion of the exciton states are relevant for a given problem.

3.2.3 Systems with electrical contacts

Another issue when probing optoelectronic structures is the need to account for injection from electrical contacts, i.e. when the semiconductor has open spatial boundaries to exchange charge carriers with an environment (e.g. for investigation of free carrier external field induced drift velocity optical nonlinearities). Contact or injection model problems are natural ingredients in methods arising from transport theory, e.g. non-equilibrium Greens functions, Wigner formalism, and Monte Carlo methods. As we have already mentioned, such methods are also used to analyze short pulse laser experiments. SBE, on the other hand, is a theory that has appeared directly from the analysis of optical experiments, and carrier injection/open boundaries have obviously not been the primary concern.

In nanoscale devices both coherent - i.e. scattering-free - and incoherent - i.e., phase-breaking -processes must be treated simultaneously. In spite of the quantum mechanical behavior of carrier dynamics in the device active region, the overall behavior is often the result of an interaction between phase coherence and energy relaxation/dephasing, the latter being primarily due to the presence of spatial boundaries or contacts/charge

reservoirs. A microscopic theory for the description of quantum-transport phenomena in systems with open boundaries was proposed by (Proietti Zaccaria & Rossi, 2003). They showed that the application of the conventional Wigner-function quantum transport formalism to this problem leads to unphysical results, such as injection of coherent electronic states from the contacts. A generalization of the Wigner-function formulation was made, able to describe both the active region and the incoherent nature of carrier injection more akin to the phenomenological injection models already used for open quantum devices.
A generalization to systems with open boundaries of the SBE has also been proposed (Rossi, 1998). However, the emphasis was mainly on phase coherence and energy relaxation within the active region, and to a lesser extent on the carrier-injection from the electrical contacts into the device.

3.2.4 Semiconductor Luminescence Equations (SLE)

Recombination of electron-hole pairs and luminescence are fundamental processes in semiconductors. The luminescence in atomic systems is modified when atoms are optically coupled or when they are located within a cavity. With an array of quantum wells a similar case can be established for semiconductors. Radiation from individual QWs is partially reflected, transmitted, or absorbed by the neighbors. By placing the quantum wells in a semiconductor microcavity, further modifications occur. For low photon energy excitations the semiconductor material shows excitonic resonances below the fundamental absorption edge. In a microcavity designed so that the exciton resonance is strongly coupled to the single longitudinal cavity mode one obtains a double peaked mode coupling spectrum which is revealed in transmission, reflection, and photoluminescence. Like in atomic systems, strong coupling effects and suppressed or enhanced spontaneous emission are a result of the high-quality optical resonance.
Pump-probe experiments can usually be explained in sufficient detail by a classical description of the electromagnetic field. A quantum treatment only leads to small corrections as long as the classical fields exceed the vacuum fluctuations. Therefore a full quantum theory of radiation interacting with semiconductor materials is necessary only in situations where these fluctuations really make a difference. Experimentally this is the case for the analysis of luminescence, i.e., for radiation spontaneously emitted when excited electrons return from the conduction to the valence band (radiative electron-hole recombination). Spontaneous emission is a pure quantum effect and no classical radiation field needs to be present. Analysis of statistical properties and correlations of the electromagnetic field requires a full quantum theory as well. A study of luminescence properties together with the presence of classical fields should therefore both be challenging and give valuable insight into the coupling of matter and radiation.
Within a classical description of radiation, a major problem arises from the consistent inclusion of carrier-carrier Coulomb interactions. Excitonic effects manifest themselves through inclusion of the Coulomb interaction between carriers. In this review, a theory for the semiconductor luminescence of electron-hole pairs is presented which includes many-body effects. We shall treat the interacting carrier-photon system in the electron-hole picture. The operator equations are presented for the case of a single quantum well (QW), but the theory is part of a more general approach for investigating quantum properties of radiation in semiconductors. The theory is valid both in the linear and nonlinear regimes

and can be used not only to analyze stationary emission under quasi-steady state conditions but also for the temporal emission in transient non-equilibrium situations. Mixing of incoherent and coherent fields can also be investigated. In the presentation by Kira et al. (Kira et al., 99), further results explaining the emission of radiation from single-quantum wells, quantum-well arrays, and quantum wells inside high-finesse optical cavities are summarized.

Here we shall mainly concentrate on incoherent luminescence resulting from a population of excited electrons and holes. As a consequence of the attractive interband interaction, strong correlations between conduction-band electrons and valence-band holes are to be expected. We have already mentioned earlier that for low excitation densities and low carrier temperatures these correlations lead to excitonic (bound electron-hole pair) resonances below the fundamental absorption edge, and that these resonances often dominate the absorption and emission spectra. The semiconductor luminescence equations (SLE) provide a description of incoherent excitonic photoluminescence. They are based on a generalization of the Hartree-Fock decoupling scheme and lay the foundations for relations between photoluminescence and absorption, the build-up of radiation from excitons, and nonlinear radiation effects. The equations bear some resemblance to the semiclassical Semiconductor Bloch equations describing the coherent excitation dynamics.

When coherent sources resonantly excite the QW (optical pumping), we have to extend the analysis to include also a classical driving field. In this case the semiconductor luminescence equations are coupled to the semiconductor Bloch equations leading to a mixing of coherent excitation and luminescence. So, in essence, coherent field effects are described classically, and incoherent field effects are treated quantum mechanically. A typical situation where the SLE can be used is after an ultrashort laser pulse has excited electrons high up in the conduction band, and we want to study the luminescence in a narrow spectral region near the exciton peaks which appears as the hot electrons have cooled down. The SLE equations for a quantum well in the absence of a coherent driving field, following the notation of Kira et al. (Kira et al., 1999) are,

$$\begin{aligned} i\hbar\frac{\partial}{\partial t}\left\langle b^{+}_{q_z,\boldsymbol{q}_\parallel} b_{q'_z,\boldsymbol{q}_\parallel}\right\rangle &= \hbar\left(\omega_{\boldsymbol{q}'}-\omega_{\boldsymbol{q}}\right)\left\langle b^{+}_{q_z,\boldsymbol{q}_\parallel} b_{q'_z,\boldsymbol{q}_\parallel}\right\rangle + i\xi_{\boldsymbol{q}} u_{QW,\boldsymbol{q}}\left\langle b_{\boldsymbol{q}'} P^{+}_{QW}\left(\boldsymbol{q}_\parallel\right)\right\rangle \\ &\quad + i\xi_{\boldsymbol{q}'} u^{*}_{QW,\boldsymbol{q}}\left\langle b^{+}_{\boldsymbol{q}} P_{QW}\left(\boldsymbol{q}'_\parallel\right)\right\rangle \end{aligned} \tag{5}$$

$$\begin{aligned} i\hbar\frac{\partial}{\partial t}\left\langle b^{+}_{q_z,\boldsymbol{q}_\parallel} P_{\boldsymbol{k}_\parallel}\left(\boldsymbol{q}_\parallel\right)\right\rangle &= \left[\varepsilon^{c}_{\boldsymbol{k}_\parallel+\boldsymbol{q}_\parallel}-\varepsilon^{v}_{\boldsymbol{k}_\parallel}-\hbar\omega_{\boldsymbol{q}}-\Sigma\left(\boldsymbol{k}_\parallel,\boldsymbol{q}_\parallel\right)\right]\hbar\left(\omega_{\boldsymbol{q}'}-\omega_{\boldsymbol{q}}\right)\left\langle b^{+}_{\boldsymbol{q}} P_{\boldsymbol{k}_\parallel}\left(\boldsymbol{q}_\parallel\right)\right\rangle \\ &\quad -\left(1-f^{e}_{\boldsymbol{k}_\parallel+\boldsymbol{q}\parallel}-f^{h}_{\boldsymbol{k}_\parallel}\right)\Omega_{ST}\left(\boldsymbol{k}_\parallel,\boldsymbol{q}\right)+f^{e}_{\boldsymbol{k}_\parallel+\boldsymbol{q}_\parallel} f^{h}_{\boldsymbol{k}_\parallel}\Omega_{SE}\left(\boldsymbol{q}\right) \end{aligned} \tag{6}$$

$$i\hbar\frac{\partial}{\partial t} f^{e}_{\boldsymbol{k}_\parallel} = 2i\sum_{q_z,\boldsymbol{q}_\parallel}\mathrm{Im}\left[-i d^{*}_{cv}\left(\boldsymbol{q}_\parallel\right)\xi_{\boldsymbol{q}} u^{*}_{QW,\boldsymbol{q}}\left\langle b^{+}_{q_z,\boldsymbol{q}_\parallel} P_{\boldsymbol{k}_\parallel-\boldsymbol{q}_\parallel}\left(\boldsymbol{q}_\parallel\right)\right\rangle\right] \tag{7}$$

$$i\hbar\frac{\partial}{\partial t} f^{h}_{\boldsymbol{k}_\parallel} = 2i\sum_{q_z,\boldsymbol{q}_\parallel}\mathrm{Im}\left[-i d^{*}_{cv}\left(\boldsymbol{q}_\parallel\right)\xi_{\boldsymbol{q}} u^{*}_{QW,\boldsymbol{q}}\left\langle b^{+}_{q_z,\boldsymbol{q}_\parallel} P_{\boldsymbol{k}_\parallel}\left(\boldsymbol{q}_\parallel\right)\right\rangle\right] \tag{8}$$

where the renormalized free-particle energy is given by the expression

$$\Sigma\left(\boldsymbol{k}_{\|},\boldsymbol{q}_{\|}\right)=\sum_{\boldsymbol{k}_{\|}^{'}}\mathrm{V}_{\boldsymbol{k}_{\|}-\boldsymbol{k}_{\|}^{'}}\left(\mathrm{f}^{\mathrm{e}}_{\boldsymbol{k}_{\|}^{'}+\boldsymbol{q}_{\|}}+\mathrm{f}^{\mathrm{h}}_{\boldsymbol{k}_{\|}^{'}}\right) \tag{9}$$

with

$$\mathrm{V}_{\boldsymbol{k}_{\|}}=\frac{\mathrm{e}^2}{2\varepsilon_0\left|\boldsymbol{k}_{\|}\right|}\int\mathrm{g(z')g(z)e}^{-\boldsymbol{k}_{\|}\left|\mathrm{z}-\mathrm{z}'\right|}\mathrm{dzdz}' \tag{10}$$

and where $\mathrm{g(z)}$ is the quantum-well confinement function (product of the envelope functions of the electrons in the conduction and valence bands), the (b^{+}/b) are photon creation/annihilation operators, $\xi_{\boldsymbol{q}}=\sqrt{\frac{\hbar\omega_q}{2\varepsilon_0}}$, $\mathrm{u}_{\mathrm{QW},\boldsymbol{q}}=\int\mathrm{g(z)u}_q\mathrm{(z)dz}$ with $\mathrm{u}_q\mathrm{(z)}$ and ω_q denoting the stationary radiation eigenmode amplitude and frequency, respectively. A QW polarization can then be defined by

$$\mathrm{P}_{\mathrm{QW}}\left(\boldsymbol{q}_{\|}\right)=\sum_{\boldsymbol{k}_{\|}}\left[\boldsymbol{d}^{*}_{\mathrm{cv}}\mathrm{P}_{\boldsymbol{k}_{\|}}\left(\boldsymbol{q}_{\|}\right)+\boldsymbol{d}_{\mathrm{cv}}\mathrm{P}^{+}_{\boldsymbol{k}_{\|}}\left(\text{-}\boldsymbol{q}_{\|}\right)\right] \tag{11}$$

Here the electron picture is used in both the conduction and valence bands for the definition of the dimensionless operators $\mathrm{P}^{+}_{\boldsymbol{k}_{\|}}\left(\boldsymbol{q}_{\|}\right)$ and $\mathrm{P}_{\boldsymbol{k}_{\|}}\left(\boldsymbol{q}_{\|}\right)$. The conduction band electron creation/annihilation (c^{+}/c) and valence band electron creation/annihilation (ν^{+}/ν) operators define

$$\mathrm{P}^{+}_{\boldsymbol{k}_{\|}}\left(\boldsymbol{q}_{\|}\right)=c^{+}_{\boldsymbol{k}_{\|}+\boldsymbol{q}_{\|}}\nu_{\boldsymbol{k}_{\|}},\mathrm{P}_{\boldsymbol{k}_{\|}}\left(\boldsymbol{q}_{\|}\right)=\nu^{+}_{\boldsymbol{k}_{\|}}c_{\boldsymbol{k}_{\|}+\boldsymbol{q}_{\|}} \tag{12}$$

$\mathrm{P}^{+}_{\boldsymbol{k}_{\|}}\left(\boldsymbol{q}_{\|}\right)$ is a dimensionless microscopic polarization operator which creates an *electron* in the conduction band and destroys an *electron* in the valence band, i.e., it creates an electron-hole pair, whereas $\mathrm{P}_{\boldsymbol{k}_{\|}}\left(\boldsymbol{q}_{\|}\right)$ destroys (recombines) the same electron-hole pair. If this recombination occurs radiatively, the emitted photon will have momentum $\boldsymbol{q}_{\|}$. In the electron-hole picture, remembering that a hole at $\text{-}\boldsymbol{k}_{\|}$ actually represents a missing valence electron at $\boldsymbol{k}_{\|}$, the center of mass of this electron-hole pair moves with the momentum $\boldsymbol{q}_{\|}$. The actual dipole density can now be written as a sum over the electron-hole pair momenta $\boldsymbol{q}_{\|}$

$$\mathrm{P}(\boldsymbol{r})=\frac{1}{\Lambda}\sum_{\boldsymbol{q}_{\|}}\mathrm{P}_{\boldsymbol{QW}}\left(\boldsymbol{q}_{\|}\right)\mathrm{e}^{-\mathrm{i}\boldsymbol{q}_{\|}\cdot\boldsymbol{r}_{\|}}\mathrm{g(z)} \tag{13}$$

Where, as mentioned above, $\mathrm{g(z)}$ is the quantum-well confinement function (product of the envelope functions of the electron in the conduction and valence bands), and Λ is the quantum well normalization area. This represents a closed set of equations with the renormalized stimulated contribution

$$\Omega_{ST}\left(\boldsymbol{k}_{\|},\boldsymbol{q}\right) = \mathrm{d}_{cv}^{*}\left(\boldsymbol{q}_{\|}\right)\left(\sum_{q'z}\left[\mathrm{i}\xi_{\boldsymbol{q}'_z,\boldsymbol{q}_{\|}}\mathrm{u}_{QW,q'_z,\boldsymbol{q}_{\|}}\left\langle \mathrm{b}_{\boldsymbol{q}}^{+}\mathrm{b}_{\boldsymbol{q}_z,\boldsymbol{q}_{\|}}\right\rangle - \frac{\mathrm{g}_{QW}}{\varepsilon_0 \mathrm{n}^2 \Lambda}\sum_{\boldsymbol{k}'_{\|}}\mathrm{d}_{cv}^{*}\left(\boldsymbol{q}_{\|}\right)\left\langle \mathrm{b}_{\boldsymbol{q}}^{+}\mathrm{P}_{\boldsymbol{k}'_{\|}}\left(\boldsymbol{q}_{\|}\right)\right\rangle\right]\right) + \sum_{\boldsymbol{k}'_{\|}}\mathrm{V}_{\boldsymbol{k}'_{\|}-\boldsymbol{k}_{\|}}\left\langle \mathrm{b}_{\boldsymbol{q}}^{+}\mathrm{P}_{\boldsymbol{k}'_{\|}}\left(\boldsymbol{q}_{\|}\right)\right\rangle \tag{14}$$

where $g_{QW} = \int g(z)g(z)dz$ and n is the quantum well index of refraction. In $\Omega_{ST}\left(\boldsymbol{k}_{\|},\boldsymbol{q}\right)$ the first term is a source term due to field correlations and the second and third terms describe its renormalization due to the dipole self-energy and the Coulomb interaction, respectively. In the SLE equation describing the radiation-matter correlation $\left\langle \mathrm{b}_{\boldsymbol{q}}^{+}\mathrm{P}_{k_{\|}}\right\rangle$ the term proportional to $1-\mathrm{f}^{e}_{\boldsymbol{k}_{\|}+\boldsymbol{q}_{\|}}-\mathrm{f}^{h}_{\boldsymbol{k}_{\|}}$ represents either absorption or stimulated emission depending on the carrier occupation of the various quantum well electronic states. The strength of the spontaneous emission,

$$\Omega_{SE}\left(\boldsymbol{q}\right) = \mathrm{i}\xi_{\boldsymbol{q}}\mathrm{u}_{QW,\boldsymbol{q}}\mathrm{d}_{cv}\left(\boldsymbol{q}_{\|}\right) \tag{15}$$

is determined by the dipole matrix element d_{cv} and the effective mode strength u_{QW_q}. The term $\left\langle \mathrm{b}_{\boldsymbol{q}}^{+}\mathrm{P}_{k_{\|}}(q_{\|})\right\rangle$ represents an electron-hole pair with center of mass momentum $\hbar q_{\|}$ recombining by emitting a photon with the same in-plane momentum $q_{\|}$. When excited carriers are present in the QW, this correlation builds up even if the field-particle and the field-field correlations are initially absent, because the source term $\mathrm{f}^{e}_{\boldsymbol{k}_{\|}+\boldsymbol{q}_{\|}}\mathrm{f}^{h}_{\boldsymbol{k}_{\|}}\Omega_{SE}\left(\boldsymbol{q}\right)$ in the equation is nonzero. Thus, $\left\langle \mathrm{b}^{+}_{q_z,\boldsymbol{q}_{\|}}\mathrm{P}_{\boldsymbol{k}_{\|}}\left(\boldsymbol{q}_{\|}\right)\right\rangle$ describes spontaneous photon emission and electron-hole recombination.

Considering the product $\mathrm{f}^{e}_{\boldsymbol{k}_{\|}+\boldsymbol{q}_{\|}}\cdot\mathrm{f}^{h}_{\boldsymbol{k}_{\|}}$, spontaneous recombination occurs only if an electron at $k_{\|}+q_{\|}$ and a hole at $k_{\|}$ are simultaneously present. As field correlations begin to build up, the stimulated contribution $\Omega_{ST}\left(\boldsymbol{k}_{\|},\boldsymbol{q}\right)$ becomes able to influence the photoluminescence spectrum. What we observe as photoluminescence is therefore a result of an interaction of field-field and field-particle correlations affected by both spontaneous and stimulated emission.

Luminescence is connected to the carrier and photon-number operators of the system. The total change in photon and carrier numbers follow from the SLE as

$$\frac{\partial}{\partial t}\sum_{\boldsymbol{q}}\left\langle \mathrm{b}_{\boldsymbol{q}}^{+}\mathrm{b}_{\boldsymbol{q}}\right\rangle = -\sum_{\boldsymbol{k}_{\|}}\mathrm{f}^{e,h}_{\boldsymbol{k}_{\|}} \tag{16}$$

meaning that any time an electron and a hole recombines radiatively, a photon is emitted.

Regarding spontaneous emission as the source of the photoluminescence, a reasonable question at this stage would be whether or not radiation field modes of different in-plane momentum $q_{\|}$ can be coupled. It turns out that within the Hartree-Fock approximation, spontaneous emission from an incoherent carrier distribution (we call this incoherent

spontaneous emission) is only allowed when the recombining electron-hole pair and the emitted photon have the same in-plane momentum. Therefore photoluminescence from different $q_{||}$ can couple only via the carrier-occupation dynamics.
If, in addition to the spontaneous component there is a non-zero coherent (optical pumping) component, quantum correlations of the type

$$\Delta\left\langle b^{+}_{q_z,\boldsymbol{q}_{||}} P_{\boldsymbol{k}_{||}}(\boldsymbol{q}_{||})\right\rangle = \left\langle b^{+}_{q_z,\boldsymbol{q}_{||}} P_{\boldsymbol{k}_{||}}(\boldsymbol{q}_{||})\right\rangle - \left\langle b^{+}_{q_z,\boldsymbol{q}_{||}}\right\rangle\left\langle P_{\boldsymbol{k}_{||}}(\boldsymbol{q}_{||})\right\rangle \tag{17}$$

will contain coherent contributions from both the semiconductor Bloch equations as well as from the incoherent processes described by the semiconductor luminescence equations. When the coherent component is absent initially, it can be shown that the expectation values of the field and polarization operators in the second term on the RH side of the above equation are zero, and in this case the SLE given above directly gives the expectation value of the correlation.
Stimulated emission also conserves the in-plane momentum, meaning that modes with different in-plane momentum do not couple radiatively. We just saw that this also holds for spontaneous emission. Incoherent photoluminescence is thereby greatly simplified, since field-field and field-matter correlations only contain quantities with the same $q_{||}$. Thus, in summary, photoluminescence contributions with different $q_{||}$ can only affect each other via the carrier-occupation.
Under stationary optical pumping the analysis could become even simpler since electron-hole pairs lost due to recombination are replaced by the pump, keeping carrier occupations constant. But coherent pumping introduces additional correlation terms leading to a coupling of modes with different $q_{||}$, which is discussed in Kira et al. (Kira et al., 1999).

3.2.5 Plasmons and coupled plasmon LO phonon effects

Charge-density waves (plasmons) in the carrier ensemble and lattice vibrations (phonons) are basic collective excitations in solids. In polar semiconductors, longitudinal optical (LO) phonons carry long range electric fields which couple to the electric fields of the longitudinal charge-density waves. Plasmons and LO phonons then form two new hybrid modes at different frequencies. This phenomenon was first observed by incoherent Raman scattering of continuous laser radiation from GaAs (Mooradian & Wright, 1966). The LO phonon-plasmon coupled hybrid excitations exhibit fundamentally different properties compared to the bare resonances. The mixed resonances still convey the carrier-carrier as well as the carrier-lattice interaction. Therefore, they are of fundamental importance for transport and relaxation dynamics in polar materials.
Free carriers in semiconductors can be introduced either by doping or by optical excitation. Under optical excitation, both electrons and holes appear simultaneously. Because of the large mass of heavy holes compared to conduction band electrons, holes can often be viewed as stationary while electrons are subjected to the plasmon oscillation.
The longitudinal mode frequencies of the coupled plasmon-phonon system are zeros of the total dielectric response function in the weak damping, long wavelength limit, i.e., where (Ridley, 1999)

$$\varepsilon_T = \varepsilon_L + \varepsilon_e - \varepsilon_0 = 0 \tag{18}$$

The free space permittivity ε_0 is subtracted once to avoid double counting, as it is included in both the lattice permittivity ε_L and the electronic permittivity ε_e. These can be given as simple Drude models,

$$\varepsilon_{\mathrm{L}} = \varepsilon_{\infty} \frac{\omega^2 - \omega_{\mathrm{LO}}^2}{\omega^2 - \omega_{\mathrm{TO}}^2} \tag{19}$$

$$\varepsilon_{\mathrm{e}} = \varepsilon_0 - \frac{\omega_{\mathrm{P}}^2}{\omega^2} \tag{20}$$

Here ω_{LO} and ω_{TO} are the longitudinal optical and transverse optical bare phonon frequencies, with the bare plasmon frequency for a carrier density n defined as $\omega_p^2 = ne^2/m^*\varepsilon_\infty$. The trick of defining an optical effective mass m^* accounts for a non-parabolic conduction band; m^* is essentially a fitting parameter which changes as the doping density increases. The result is that the longitudinal phonon mode and pure plasmon mode are replaced by the two coupled modes designated by ω_+ and ω_-. Their frequencies are given by

$$\omega^4 - \omega^2\left(\omega_{\mathrm{LO}}^2 + \omega_{\mathrm{P}}^2\right) + \omega_{\mathrm{TO}}^2\omega_{\mathrm{P}}^2 = 0 \tag{21}$$

In Fig. 3 we have calculated the eigenfrequencies for the two hybrid modes ω_+ and ω_- in $Cd_{0.28}Hg_{0.72}Te$ as a function of carrier density at long wavelengths ($\boldsymbol{q} \sim \mathbf{0}$) of the modes. We notice that at low carrier densities the upper mode ω_+ resembles a bare LO phonon mode with a fixed resonance frequency, whereas the lower mode ω_- resembles a bare plasmon with a linearly increasing resonance frequency as a function of carrier density. At low carrier densities the oscillation period of the plasmon is very long, but at higher carrier densities its oscillation period starts to approach that of the LO phonon-like upper mode. At this level of carrier density the effect of mode coupling becomes strong, and must be accounted for when dealing with transport problems or relaxation dynamics. This coupling region is in fact the most difficult domain to model. If the carrier density is increased even more, the upper mode changes character and becomes plasmon-like while the lower mode becomes LO phonon like. Again, we have a plasmon-like and a LO phonon-like mode, but now it is the upper hybrid mode that is plasmon-like and the lower hybrid mode that is LO phonon-like. A small artefact with the lower hybrid mode clearly seen in the figure is that it oscillates at the *tranverse* optical phonon frequency at high carrier densities, rather that at the LO phonon frequency. LO phonons generally have a larger restoring force than do TO phonons, and they therefore oscillate at a slightly higher frequency. This difference is due to the long range electric field that LO phonons carry. At high carrier densities this field is (over)screened by the now rapidly oscillating plasmon charge carriers, and thus the oscillation will occur at (or below) the bare TO frequency.

The physics described above is based on an assumption of quasi steady-state or quasi equilibrium. We know that oscillating charge carriers generally emit radiation. If the material can be brought far away from thermal equilibrium, radiation from the hybrid modes should become clearly discernible. In addition, the formation time from bare resonances to the fully developed hybrid modes could be revealed if the number of charge

carriers is suddenly increased from a very low value to a value where coupling is expected to occur.

We shall first deal with the issue of radiation from the hybrid modes, that is, free-space radiation originating from longitudinal modes of a polar semiconductor as a function of coupling. It is perhaps to be expected that plasmons are the strongest radiators, and that the radiation spectrum is only significantly disturbed when entering the coupling region. If the semiconductor is excited with a short laser pulse, we readily obtain an inhomogeneous, hot electron-hole plasma. A colder, well thermalized plasmon-phonon hybrid would clearly be a more ideal object of study. Therefore the sample should have a background donor doping (giving an n-type semiconductor) in which the colder plasmon-phonon hybrid can be established. Steady-state non-equilibrium of this colder hybrid is ensured if it is interacting with a hot, laser-induced electron-hole plasma. The density of the hot plasma can be several orders of magnitude higher than the background doping density. Interactions between the cold hybrid mode and the laser-induced hot plasma are rather subtle. Samples for this kind of experiments have a surface space-charge region. An ultrashort laser pulse creates electron-hole pairs, suddenly screening out the surface field. Higher doping density results in a shorter space-charge layer, resulting in faster screening of the surface field. Coulomb coupling of the ultrafast surface field transient to both the electronic and the lattice subsystems then initiate the collective oscillations which form the hybrid modes. Both

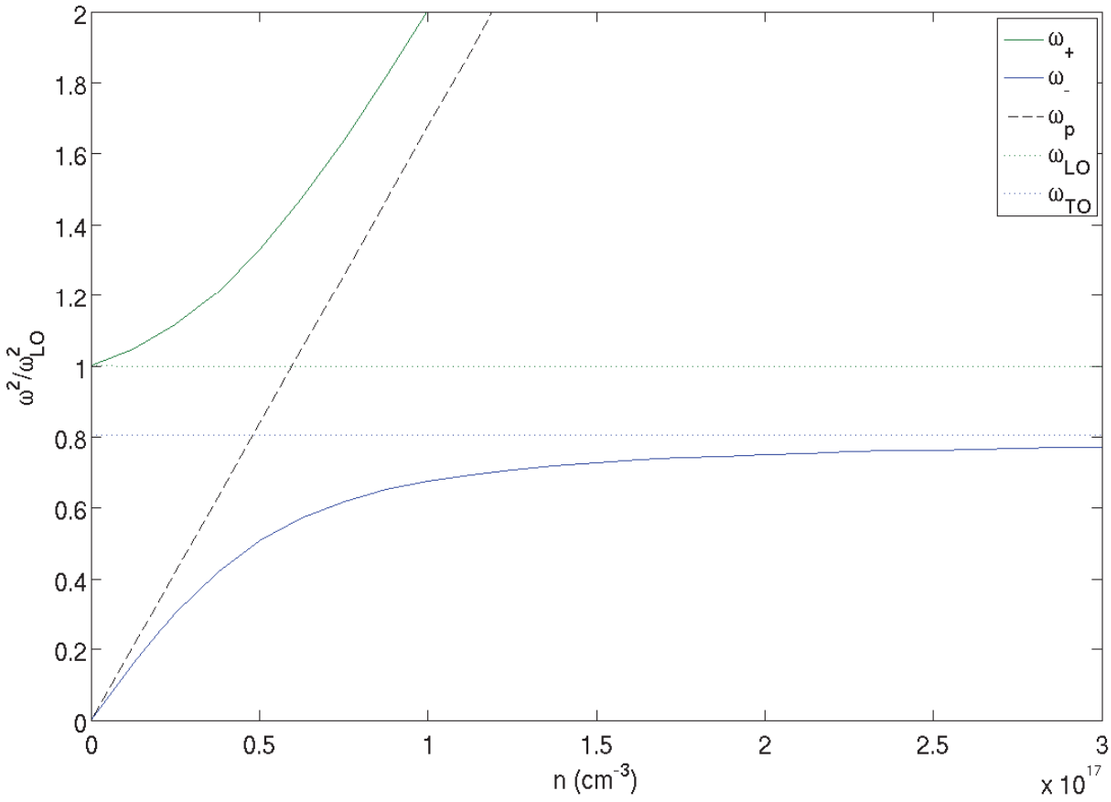

Fig. 3. A plot of the frequencies associated with the hybrid modes. Calculations done for $Cd_{0.28}$ $Hg_{0.72}Te$ at 300 K. The band gap is 0.271 eV.

components of the cold hybrid mode have intrinsic damping rates, for LO phonons a decay time of 1-2 ps describes the disintegration of the LO mode into acoustic phonon modes, and for electrons sub-ps momentum relaxation times connected to various carrier scattering processes define the damping rate of the plasmon. Presence of a hot, laser induced plasma of high density in the same sample will change the cold plasma carrier scattering rates (especially the rates concerning donor electron scattering with laser induced hot holes) and enhance the damping of the cold hybrid mode. The altered damping rates can be extracted from the radiation emitted by the hybrid mode, and compared with rates extracted from electric mobility measurements of the doped sample.

Time-resolved measurements of hybrid modes in polar semiconductors can be made by reflective electro-optic sampling (REOS) (Dekorsy et al., 2000). Charge carriers are generated by an ultrafast laser pulse, and the hybrid modes weakly modulate the surface field as observed by reflection. Among the drawbacks of REOS is a lack of sensitivity to oscillations beyond the surface field layer and less distinction between photocarrier and background doping carrier densities.

Two other detection techniques are optically gated antennas and free-space electro-optic sampling, which give the phase of the THz pulse relative to the excitation pulse. Phase data can in principle reveal details of the starting mechanism of the hybrid oscillations, but they are technically difficult to obtain due to dispersion and absorption effects in the semiconductor (Leitenstorfer et al,. 1999, Kono et al., 2000).

Ignoring this phase information, Hasselbeck et al. (Hasselbeck et al., 2002) used a broadband interferometric method with two 30 fs pump pulses directed at nearby regions in InAs to extract transient THz radiation signals interfering in the far field. The angle of incidence for the Ti:sapphire laser beams was 45° and the pump pulses exceeded the band gap by 1.2 eV. Excited carrier density in the pump absorption region was estimated to be $>10^{18}\mathrm{cm}^{-3}$, with an absorption depth of the pump > 200 nm, and the surface accumulation field depth was ~ 5 nm. This ensures that the pump penetrated well into the neutral bulk region where the hybrid oscillations are created. Response times of the surface field screening were 52 – 76 fs, decreasing with increased doping.

By adjusting the time-delay between the pump pulses an interferogram is created, which could be Fourier transformed and analyzed in order to extract vital data regarding the hybrid modes.

In (Kersting et al, 1997) a simple model is presented which can be used to calculate the power spectrum of the emitted THz radiation of the experiment, assuming homogeneous broadening (Hasselbeck et al., 2002);

$$\begin{aligned} \mathrm{P}(\omega) &\sim \omega^4 \left|\mathrm{E}(\omega)\right|^2 \cdot \left| \frac{\omega_\mathrm{p}^2\left(\varepsilon_\infty \mathrm{D}_1(\omega) - 4\pi\cdot\Omega\right) + \Omega\left[\mathrm{D}_2(\omega) - \omega_\mathrm{p}^2\right]}{\varepsilon_\infty \mathrm{D}_1(\omega)\mathrm{D}_2(\omega) - 4\pi\cdot\Omega\omega_\mathrm{p}^2} \right|, \\ \mathrm{D}_1(\omega) &= -\omega^2 + \mathrm{i}\gamma_{\mathrm{ph}}\omega + \omega_{\mathrm{LO}}^2 \\ \mathrm{D}_2(\omega) &= -\omega^2 + \mathrm{i}\gamma_{\mathrm{el}}\omega + \omega_\mathrm{p}^2 \end{aligned} \tag{22}$$

with $\Omega = \omega_{TO}^2(\varepsilon_s - \varepsilon_\infty)/4\pi$ (ε_s is the static dielectric constant) and γ_{ph}, γ_{el} as LO phonon decay and electron momentum relaxation rates, respectively. At the edge of the space-charge layer the surface electric field transient is modeled as $E(t) = E_0[\tanh(t/\tau)+1]$, giving $|E(\omega)|^2 \sim \mathrm{csch}^2(\pi\omega\tau/2)$, where τ is an analytic approximation to a calculated response time of the

surface field screening. The center frequencies of the spectral peaks are quite insensitive to a change in optical excitation power, since they are determined by the cold plasma density.
The laser-generated, hot charge carriers do not emit coherently due to their inhomogeneous, i.e., quasi-exponential distribution in the bulk region adjacent to the surface. Distinguishable contributions from both ω_+ and ω_- hybrid modes can be directly observed in the radiated signals. By varying the donor doping, the plasma frequency changes, and we can study the different regions of hybrid mode coupling similar to those depicted in Fig. 3.
Having discussed the emission of radiation from non-equilibrium hybrid modes, we shall now turn our attention to the formation of hybrid modes after a sudden increase in carrier density. Femtosecond laser pulses create a dense, excited carrier plasma in an intrinsic semiconductor within a time shorter than a typical oscillation cycle of the bare LO phonon and plasmon resonances. It is to be expected that the hybrid mode resonances will not be established instantaneously in such a strongly non-equilibrium situation. Transition from an LO phonon resonance to a fully coupled phonon-plasmon hybrid will be governed by many-body quantum correlations. Screened Coulomb and phonon interactions must therefore be considered self-consistently within the same approach.
We shall briefly outline the key ingredients of a quantum kinetic theory in the framework of Keldysh non-equilibrium Greens functions (Haug & Jauho, 1996). The analysis can be viewed as a generalization of the steady-state theory presented above, where we found the longitudinal hybrid eigenmode resonances as the roots of the dielectric function. Manybody system response can quite generally be obtained via the dielectric function, usually expressed via its inverse form ε^{-1} (Ridley, 1999, Mahan, 2007). For a NIR pump-THz probe experiment we are interested in the inverse dielectric function $\varepsilon_q^{-1}(t_d,\omega)$ where t_d is the delay between pump and probe, and $\boldsymbol{q}$, ω are the wavevector and frequency of the hybrid phonon-plasmon resonance, respectively. $\mathrm{Re}(1/\varepsilon_q)$ essentially describes the screening effects of the manybody system, in particular the resonant overscreening of the long range electrostatic restoring force of the LO phonon, which was seen earlier to reduce the ω_- oscillation frequency to lie below the TO phonon frequency at high carrier densities (Fig. 3). The imaginary part of the dielectric function reflects the energy loss of a carrier interacting with the many-particle system. Sustained longitudinal electromagnetic eigenmodes are identified from the peaks of $\mathrm{Im}(1/\varepsilon_q)$.
The two-time particle interaction is calculated self-consistently with the semiconductor Bloch equations, and the Dyson equation determines the effective screened interaction potential,

$$W_{\boldsymbol{q}}(1,2) = W_{\boldsymbol{q}}^{0}(1,2) + W_{\boldsymbol{q}}^{0}(1,3)L_{\boldsymbol{q}}(3,4)W_{\boldsymbol{q}}(4,2) \tag{23}$$

where the polarization function $L_q(t; t')$ is based on the random-phase approximation (RPA). The effective screened interaction potential $W_{\mathbf{q}}^{0}(1,2)$ describes the combined Coulomb interaction and the interaction due to LO phonon scattering. Exponential damping is introduced into the phonon propagator, and the corresponding two-time Greens functions are modeled according to the generalized Kadanoff-Baym ansatz. Then an incomplete Fourier transform of the resulting effective interaction potential $W_{\mathbf{q}}^{r}(t_1,t_2)$ is taken, considering the relative time $t_1 - t_2$, and the inverse dielectric function is finally obtained by setting $t_D = t_1$ (Huber et al., 2005b, Vu & Haug, 2000),

$$W_{\boldsymbol{q}}^{r}(t_1,\omega)=\int_{-\infty}^{t_1} dt_2 W_{\boldsymbol{q}}^{r}(t_1,t_2)e^{i\omega(t_1-t_2)},$$
$$\varepsilon_{\boldsymbol{q}}^{-1}(t_D,\omega)=W_{\boldsymbol{q}}^{r}(t_D,\omega)/V_{\boldsymbol{q}} \quad (24)$$

with V_q denoting the strength of the bare Coulomb interactions.

Huber et al. (Huber et al., 2005b) investigated the formation of hybrid modes in intrinsic InP using a 12-fs Ti:sapphire laser pump with a single-cycle THz probe at 28 THz, delayed with the time t_D. Real-time evolution of the probe THz electric field was directly measured by means of the ultrabroadband electro-optic sampling technique with sampling delay time t_s. The measured data allowed access to both real and imaginary parts of $\varepsilon_q(t_D,\omega)$ in a 7 - 60 THz window.

Delaying the probe with respect to the pump resulted in characteristic trailing oscillations long after the original probe signal had died out. The trailing oscillations represent a change in the probe signal which was monitored by varying the sampling delay time t_s. Increasing the delay between pump and probe resulted in more trailing oscillation cycles. These oscillation cycles are manifestations of a quantum beating between the newly developing upper and lower hybrid modes ω_+ and ω_- in Fig. 3.

The hybrid resonances can be followed by a Fourier transformation with respect to t_s of the change in the real-time probe signal for various pump-probe delays t_D, thereby extracting the inverse dielectric function $\varepsilon_q^{-1}(t_d,\omega)$ in the long wavelength limit $\boldsymbol{q} = \mathbf{0}$. For an unexcited semiconductor only the bare LO phonon resonance is found, which vanishes after photoexcitation and then two new hybrid modes arise after a while. By varying the carrier densities the position of the peaks in of $\mathrm{Im}(1/\varepsilon_{\boldsymbol{q}=\mathbf{0}})$ can be followed. As a reference, TO phonons in InP oscillate at $\omega_{TO}/2\pi = 9.7$ THz, and LO phonons at $\omega_{LO} = 10.3$ THz. In the time-domain, it was demonstrated both experimentally and theoretically that the time for establishment of fully developed hybrid modes depends on the carrier density as $\tau_H = 1.6\omega_+/2\pi$. This means that the buildup takes shorter time in denser systems, c.f. Fig 3. Typical values of τ_H for InP would be ~ 140 fs at a carrier density of $10^{18}\,\mathrm{cm}^{-3}$.

3.2.6 Magnetic systems

Diluted ferromagnetic semiconductors are currently explored for use in information processing and storage devices. By introducing Mn atoms in GaAs or other III-V semiconductors a new, ferromagnetic material is obtained in which fast spin manipulation seems possible. Other candidate material classes investigated in the literature are chrome spinels, manganese oxides, transition metals, rare earths, pyrochlore, EuO, and EuS.

Spin manipulation is a basic ingredient in spintronics, spin-photonics and quantum computation applications. Carrier density induced ferromagnetic effects can either be controlled by light or current via electrical contacts and gates. Magnetic field pulses and spin-currents can control the spin on the picosecond timescale, but for femtosecond manipulation, ultrashort laser pulses will have to be introduced. For the investigation of candidate materials a particular experimental method is used, ultrafast pump-probe magneto-optical spectroscopy. Here the pump optical pulse creates carrier populations

whose subsequent interactions starts the magnetization dynamics which can be followed as a function of time via Faraday or Kerr rotation.

Natural timescales for phonon mediated spin relaxation and magnetization precession lie in the picosecond range. This was considered to be the ultimate limit for the attainable speed of magnetization switching prior to investigations with fs pulsed lasers. Then ultrafast demagnetization with the aid of fs lasers was demonstrated and this opened up new possibilities for high-speed magnetic devices. We shall first consider the metals because a large body of results has been obtained here and the corresponding theory has matured considerably in the last few years.

The ultrafast demagnetization process seen in transition metals such as Ni, Co, Fe (delocalized magnetism of *d*-electrons) and the rare-earth metal Gd (magnetism of *f* -electrons), is related to three characteristic timescales: 1) a femtosecond demagnetisation with timescale τ_E , 2) a picosecond magnetization recovery with timescale τ_M, and 3) a hundred picosecond-nanosecond magnetization precession.

Finding a satisfactory theory from first principles of the ultrafast physics going on under 1) is not straightforward. Instead, it seems at the moment more profitable to start with simpler models in order to describe the influences of the different subsystems (charge carriers, spin, photons, and phonons). For example, it is known that spin-orbit interactions are important, but modeling of all three temporal regimes on the same footing is currently not possible using quantum theory.

Early attempts assumed a three-temperature (3T) phenomenological model with rate equations for electron, phonon, and spin temperatures (energies). Using a spin temperature is quite unsatisfactory, considering that the spin system is not in equilibrium on the femtosecond timescale. If the spin is instead coupled to a two-temperature (2T) model for phonon and electron temperatures, we can obtain some improvement. Such a model deals with an energy flow concept, interpreting the ultrafast demagnetization as a non-coherent, "thermal" process. The energy goes from photon to electron and then to the spin system, without the need for stating any underlying quantum mechanism behind the spin flip.

Among the candidates for underlying quantum mechanisms are Elliott-Yafet (EY) electron-phonon scattering, EY electron scattering with impurities or other electrons and the electron-electron inelastic exchange scattering. The EY model for phonon scattering seems to be a strong candidate in many of the metals.

Further progress in the field of phenomenological models (Atxitia & Chubykalo-Fesenko, 2010) has resulted in three central branches: 1) Langevin dynamics based on the Landau-Lifshitz-Gilbert (LLG) equation and classical Heisenberg Hamiltonian for localized atomic spin moments, 2) the Landau-Lifshitz-Bloch (LLB) micromagnetics model, and 3) the Koopmans's magnetization dynamics model (M3TM).

The LLB model includes the dynamics governed by both the atomistic LLG model and the M3TM model, with both classical and quantum versions. The LLB equation for a quantum spin *S* is based on the density matrix approach. For simple quantum spin systems modeled a s a two level system with spin-up and spin-down bands (i.e. $S = \pm 1/2$) it has been shown to be equivalent to the M3TM model (Atxitia & Chubykalo-Fesenko, 2010). The LLB equation for classical spins is equivalent to an ensemble of exchange-coupled atomistic spins modeled by LLG equations.

Quantum mechanisms responsible for the ultrafast demagnetization in the LLB model are described by the coupling parameter λ, which defines the rate of the spin flip. Relations

between such parameters in the phenomenological models are a key to understand whether or not a given mechanism can act on more than one of the three characteristic timescales of the demagnetization process mentioned above.

The LLB equation can handle large spatial scales, which is a prerequisite for modeling multiscale magnetization dynamics. Coupling the spin to the electron temperature from the 2T model, we automatically include a purely carrier-based spin flip process. If both electron and phonon temperatures are coupled to the spin dynamics we automatically include the carrier-phonon scattering induced Elliott-Yafet mechanism. Coupled to the 2T model, the LLB equation has recently been shown to describe correctly all three stages of the ultrafast demagnetization processes: the sub-picosecond demagnetization, the picosecond magnetization recovery and the nanosecond magnetization precession (Atxitia & Chubykalo-Fesenko, 2010).

As regards semiconductors, similar magnetization effects have been demonstrated (Kapetanakis et al., 2009). Using density matrix equations of motion a nonequilibrium theory of ultrafast magnetization reorientation in ferromagnetic (Ga,Mn)As was presented. Interactions and coherent nonlinear optical effects were treated in a similar way as the Semiconductor Bloch equations. Both resonant and non-resonant photoexcitation were included, taking into account the relevant bands. A femtosecond collective spin tilt was induced by nonlinear, near-ultraviolet (3 eV), coherent photoexcitation with linearly polarized light. The magnetization was initiated by the interaction of non-thermal itinerant carriers (holes) with local Mn spins. The dynamics generated a subsequent uniform magnetic precession. This was interpreted as a possibility of non-thermal magnetization control by tuning the laser frequency and polarization direction.

3.3 Incoherent ultrafast regime

We shall now consider ultrafast phenomena after coherence has been completely destroyed by scattering. This is the particular branch of scattering dominated carrier relaxation dynamics which is representative for traditional micreoelectronics devices.

When electrons are photoexcited high into the conduction band, scattering processes are initiated and the initial configuration of excited charge carriers in the bands starts to change. First the charge carriers thermalize among themselves within 1 ps due to carrier-carrier scattering. Thermalization means that the charge carriers obtain a common temperature which is different from the lattice temperature. Then the cooling of the carriers towards the lattice temperature starts, and this can take tens to hundreds of picoseconds depending on the amount of photoexcited carriers and how high above the band gap the electrons were excited. Screening of the carrier-phonon scattering mechanisms at high photoexcitation densities can reduce the energy transfer rate to the lattice. Considerable feedback from the lattice to the carriers are related to bottleneck effects when the most active phonon types receive too much energy in a short time. These hot phonons obtain much higher temperatures than the less active phonons, which tend to have temperatures very close to the initial lattice temperature. Usually the energy of the pump pulse is very small in these kinds of experiments, so the hot phonons are essentially due to poor energy distribution between different phonon modes. Consequences of having hot phonons are a substantially prolonged carrier cooling time. After the cooling has resulted in equilibration of carrier and lattice temperatures, a final ‘condensation’ process where electrons and holes recombine completes the photoexcitation cycle. Before

we embark on a study of the carrier cooling and hot phonon effects, we shall investigate another type of condensation. As the photoexcited carriers start to cool, the free carrier electron-hole pairs begin to condensate into excitons. Both excitions and free electron-hole pairs have rather long lifetimes, often in the μs range. Recombination can happen within a free electron-hole pair or go via exciton recombination.

The Saha equation (Kaindl et al., 2009, Suzuki & Shimano 2011), gives the equilibrium ratio between the density of excitons N_{ex} and free carriers (i.e. when these two populations are reciprocally thermalized) in the Boltzmann limit. For bulk materials it reads,

$$\frac{N_{eh}^2}{N_{ex}} = \frac{1}{4}\left(\frac{2\mu k_B T_c}{\hbar\pi}\right)^{\frac{3}{2}} e^{\left(-E_0 / k_B T_c\right)} \tag{25}$$

where μ and E_0 are the exciton reduced mass and the binding energy, respectively. For a given total *e-h* pair density $N = N_{eh} + N_{ex}$, it yields the relationship between carrier temperature T_c and free-carrier density N_{eh}.

Free electron hole pair populations obtain thermal equilibrium with excitons within 2 ps. If we consider long timescales of some ps to hundreds of ps after the pump pulse with no external disturbance, this could be considered an instant equilibrium. The Saha equation implies that hot carriers have a low exciton density while cold carriers contain a high exciton density. However, the above equation only represents an exclusive equilibrium between free electron-hole pairs and excitons. As we saw above the carriers will still not be in equilibrium with the phonon system within a 2 ps timescale. What can happen under the carrier cooling phase is a thermal re-ionization of excitons by the phonons to create free-electron-hole pairs. The result will be a slow formation time of excitons on the order of several hundreds of ps when lattice and excitons eventually reach an equilibrium. We can consider the temporal region of carrier cooling to be free from recombination lifetime effects. After the cooling phase a final equilibrium of all subsystems is reached by recombination of excitons and free carriers.

This effect has been investigated in Si by Suzuki et al. (Suzuki & Shimano 2011) using optical pump and THz probe measurements. They evaluated the time-dependent fraction of free carriers and excitons. The waveforms of the THz pulse transmitted after the sample with and without the optical pump were recorded by electro-optic sampling. The complex transmittance change was then obtained by Fourier transformation, thereby yielding a photoinduced change in the complex dielectric function. To estimate the free *e-h* pair density at each delay time, the data were fitted with the free-carrier based Drude model in the low photon energy region (2.0–7.8 meV), where the Drude component dominates the spectrum. The Drude component decreases with increasing delay time, and an exciton component (Kaindl et al., 2009) emerged as a peak at ~ 10-12 meV, an energy that corresponds to the 1*s*-2*p* transition of excitons in Si. Thus the formation dynamics of excitons was revealed through the observation of the 1*s*-2*p* transition at ~ 3 THz. Contrary to a free-carrier behavior, the exciton density, as indicated by the 1*s*-2*p* absorption at 12 meV, gradually increased after the photoexcitation and reached a constant value after 400 ps for an initial lattice temperature of 30 K. Long after this period, recombination eventually will influence the populations.

As we have just seen, the interaction between the hot free electron-hole plasma and the phonons constitutes a very important basis for the formation of a stable exciton

population. In (Suzuki & Shimano 2011), cooling of the hot carriers was studied using a set of cooling rate expressions. A very flexible, but more computationally heavy alternative for studying this particular cooling dynamics would be to use a particle-based Monte Carlo (MC) simulation. The flexibility lies in the fact that very few assumptions have to be made about the system at hand, so that not only special cases can be considered. In the following we present some of our recent MC results in order to demonstrate the physics behind the dissipation of short laser pulses. In this case we shall investigate a low-gap semiconductor, $Hg_{0.72}Cd_{0.28}Te$ (MCT). As shown in Fig. 2, laser energy can be exchanged between carriers and phonons in several ways before finally escaping through the phonon distributions. Plots of the rate of energy exchange for $Hg_{0.72}Cd_{0.28}Te$ due to the interactions are shown in Fig. 4, for coupled MC simulations with hot phonons and exact screening.

Longitudinal optical phonons constitute the most important route for energy relaxation when carrier densities are low. Almost all the energy relaxed out of the system goes by this route, through polar optical interaction with high energy electrons. Relaxation through transversal phonons occurs via the non-polar deformation potential interaction and is usually less important.

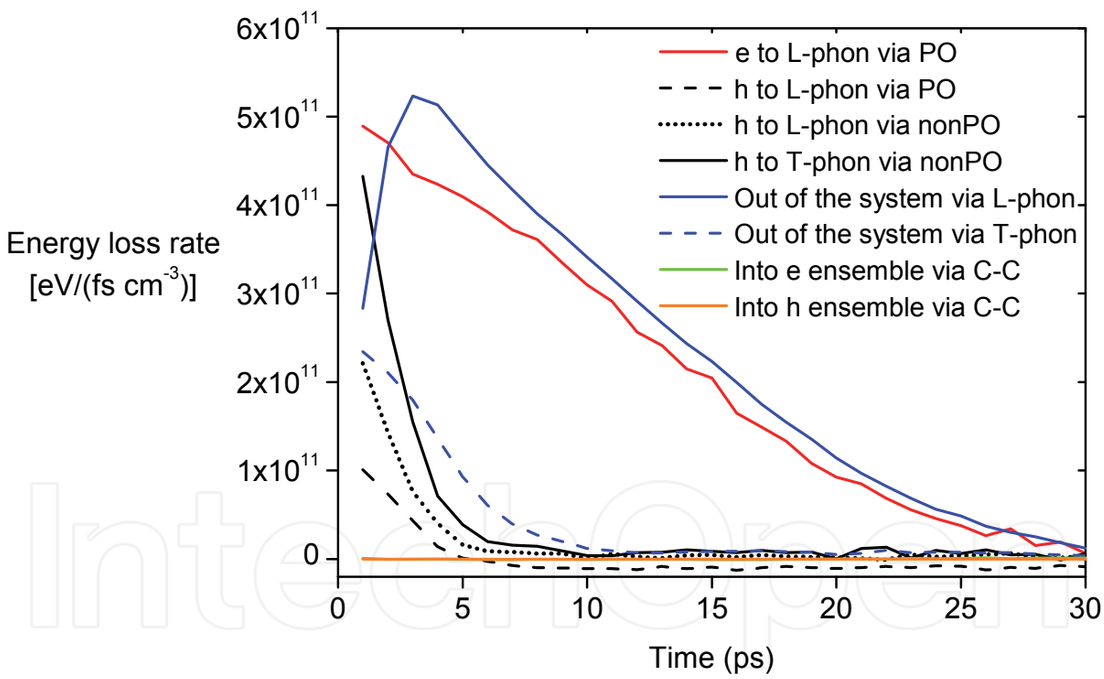

Fig. 4. Energy transfer rates of the different mechanisms at a carrier density of $n = 10^{16}\,\mathrm{cm}^3$. Hot phonons are simulated and the screening length is calculated from the simulated distributions.

We also see from the figures that the green graph representing the hole energy loss rate to longitudinal optical phonons goes slightly negative after 5 ps. This means that some energy is flowing into the hole ensemble indirectly via the mainly electron-heated hot longitudinal optical phonons. This can help energy relaxation and even out the temperature difference between electrons and holes. For the particular case investigated here however, the flow is

not large. Electrons in MCT will mainly interact with small wavevector longitudinal optical phonons, since electrons occupy a very narrow band in ***k***-space with small electron wave vectors. Thus, only longitudinal optical phonons with small wavevectors will become really "hot", as illustrated in Fig. 5.

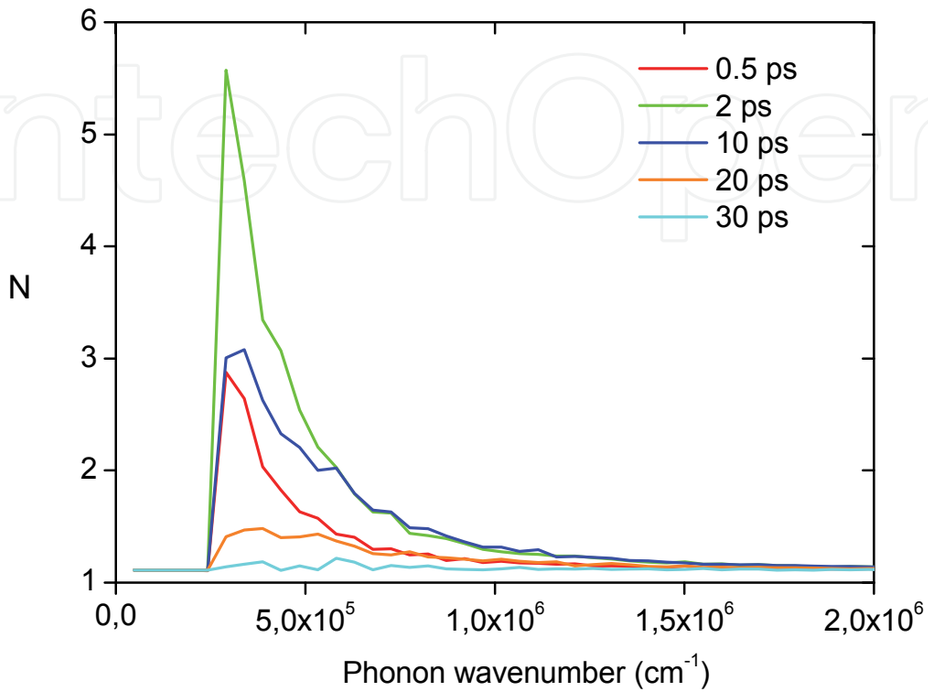

Fig. 5. Longitudinal phonon occupation at select times in simulations of coupled electron and hole ensembles at $n = 10^{16}\,\mathrm{cm}^3$, with hot phonons accounted for.

Longitudinal optical phonon modes with larger wavevectors have a phonon occupancy corresponding more closely to the lattice temperature.

Transversal phonons do not become hot either, as we can see from Fig. 6. Holes receive less of the laser energy and occupy a much broader range of wave vectors and will therefore interact with a much broader range of phonon wave vectors. Because the phonons that are hot have small wave vectors these phonons will not interact as efficiently with the broad-wavevector hole ensemble as one could expect.

At high laser fluences carrier densities will increase. Then the interaction with polar optical phonons tends to be weakened by carrier induced screening, and transversal phonons becomes a more important relaxation route. Another complication at high carrier densities and laser fluences is the occurrence of plasmons or longitudinal hybrid mode oscillations. An individual carrier can also be scattered by plasmons in elemental semiconductors such as Ge, Si etc., but not by hybrid modes.

In polar materials however, such as the compound semiconductors GaAs and MCT the plasmon mode and the longitudinal optical mode combine via their respective long range electrical fields, as we saw earlier. The combined modes replace the plasmon and polar optical mode as scattering agents of the charge carriers, and can be simulated by the same method as we have outlined here.

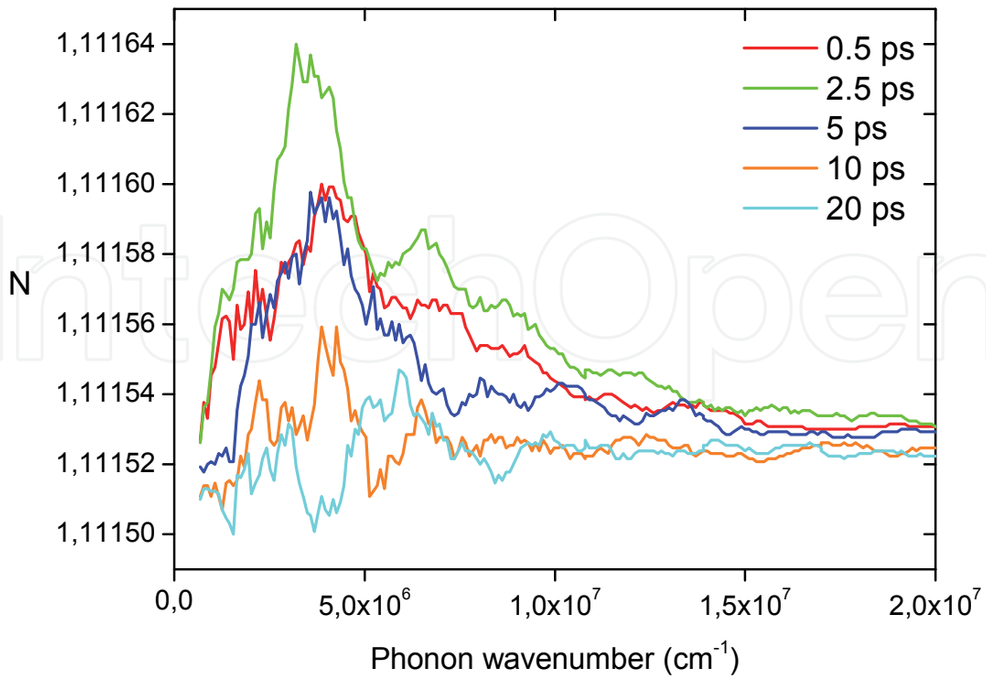

Fig. 6. Transversal phonon occupation at select times in simulations of coupled electron and hole ensembles at $n = 10^{16}\,\mathrm{cm}^3$, with hot phonons accounted for.

3.4 Long pulse regime

We shall devote some space (albeit small) also to this case, because of all the non-linear optical effects that appear. Using infrared (IR) wavelengths, intraband free carrier (FCA) and inter-valence band (IVA) absorption between e.g. the light and heavy hole bands can be studied, see Fig. 1. Although the total number of carriers generated in the conduction band can be comparable to that of a short pulse experiment, the majority of the carriers are well thermalized at temperatures which lie close to the overall lattice temperature. Nevertheless, differences between carrier and lattice temperature smaller than 100 K can have a major impact on processes occurring near the band gap, according to (Storebo et al., 2010). For example, it was found that a slightly elevated carrier temperature can strongly reduce the Pauli-induced saturation or "bleaching" of one-photon absorption across the band gap, or affect other long-timescale parameters, like carrier lifetimes and impact ionization rates. The difficulties within the modeling in this regime lies not only in the solution of many coupled differential equations, but also to a large degree on severe inaccuracies in recombination rates and TPA, FCA, IVA absorption coefficients which has now lasted for decades. The discrepancies have persisted because it has been experimentally very difficult to isolate and quantify all the simultaneous absorption and recombination effects. Theoretical estimates could be used to eliminate the uncertainties, but the methods used in the past have proven much too primitive for this task. With the advent of *ab-initio* band structure numerical codes it will become possible to obtain accurate estimates of each process, and examples of progress in this direction will become available in the near future. An important point which we would like to emphasize in this context is that even if the data is obtained numerically, it is crucial for the usefulness of the data that analytical expressions are extracted, so that the

results can be incorporated in laser irradation simulations. In addition, the data must also take into account the possibility of different carrier and lattice temperatures, a feature which we have seldom seen considered for cases involving low-intensity laser irradiation.

4. Conclusions

As we have seen, no single post evaluation tool or method will suffice to cover all pulselength ranges, and not all tools are suited for a given experiment. Combining time resolved laser experiments with satisfactory analysis of the results can therefore become a demanding task. When evaluating potential analysis tools, we will take the view that it is vital to have access to flexible methods, even if we see that this often comes at the expense of heavy numerics. It is true that the analysis of e.g. a semiconductor device by simple analytical models often benefits the physical understanding. But in the field of laser spectroscopy many processes contribute in unpredictable ways, and to have some of these ways sporadically blocked by a priori assumptions or limitations within the method of analysis can become a frustrating experience. Some of the methods reviewed in this chapter introduce substantial simplifications, and should be used, but not without focusing on their limitations and assuring the access to more flexible tools. As regards the future prospects of laser spectroscopy, it is clear that the techniques developed in this field will play a crucial role in achieving quantum coherent control of information bearing variables such as spin as well as continuing to be a central method for device and material characterization.

5. References

Ashcroft, N.W. & Mermin, N.D. (1976). *Solid State Physics*, Holt-Saunders Japan LTD, Tokyo

Atxitia U. & Chubykalo-Fesenko O. (2010). Ultra-fast magnetization rates within the Landau-Lifshitz-Bloch model. *ArXiv:1054v1 [cond-mat.mtr-sci]* (23 Nov 2010)

Axt, V.M. & Stahl, A. (1994). A Dynamics-Controlled Truncation Scheme for the Hierarchy of Density Matrices in Semiconductor Optics. *Z. Phys. B Condens. Matter*, Vol.93, pp. 195

Butov, L.V.; Lai, C.W.; Ivanov, A. L., Gossard, A.C. & Chemla, D.S. (2002). Experimental approaches for exciton Bose-Einstein condensation. *Nature*, Vol.417, pp. 47

Blanchard, F.; Sharma, G.; Razzari, L.; Ropagnol, X.; Bandulet, H.C.; Vidal, F.; Morandotti, R.; Kieffer, J.C.; Ozaki, T.; Tiedje, H.; Haugen, H.; Reid, M. & Hegmann, F. (2011). Generation of Intense Terahertz Radiation via Optical Methods. *IEEE Journal of Selected Topics in Quantum Electronics*, Vol.17, No.1, January/February 2011

Chang, E; Bussi, G.; Ruini, A & Molinari, E. (2004). Excitons in Carbon Nanotubes: An *Ab Initio* Symmetry-Based Approach. *Phys. Rev. Lett.*, Vol.92, 196401

Christensen, N.E.; Svane, A.; Cardona, M.; Chantis, A.; Laskowski, N.R.; van Schilfgaarde, M. & Kotani, T. (2011). Calculations of quasi-particle spectra of semiconductors under pressure. *Phys. Status Solidi B*, 1–6

Combescot, M.; Betbeder-Matibet, O. & Leuenberger, M.N. (2009). Analytical approach to semiconductor Bloch equations. *Europhys. Lett.*, Vol.88, 57007

Dekorsy, T.; Cho, G.C. & Kurz, H. (2000), In *Light Scattering in Solids VIII*, M. Cardona & G. Guntherodt, (Eds.), Springer

Feldtmann, T. (2009). Influence of Phonons on Semiconductor Quantum Emission, Dissertation available at

http://deposit.ddb.de/cgi-bin/dokserv?idn=999828991&dok_var=d1&dok_ext=pdf&filename=999828991.pdf

Ganichev, S.D.; Ketterl H; Prettl, W; Ivchenko, E.L & Vorbjev, L.E. (2000). Circular Photogalvanic Effect induced by Monopolar Spin Orientation in p-GaAs/AlGaAs multiple Quantum Wells. *Appl. Phys. Lett.* Vol. 77, pp. 3146

Ganichev,S.D.; Ivchenko, E.L; Danilov, S.N; Eroms, J.; Wegscheider, W,; Weiss, D. & Prettl, W. (2001). Conversion of Spin into Directed Electric Current in Quantum Wells. *Phys. Rev. Lett.,*Vol.86, pp. 4358

Ganichev, S.D.; Danilov, S.N; Bel'kov, V.V; Ivchenko, E.L; Bichler, M.; Wegscheider, W.; Weiss, D. & Prettl, W. (2002). Spin-Sensitive Bleaching and Monopolar Spin Orientation in Quantum Wells. *Phys. Rev. Lett.*, Vol.88, 057401

Griffin, C; Snoke, D.W. & Stringari, S. (1995). *Bose-Einstein Condensation*, Cambridge University Press, Cambridge, UK

Hanamura, E. & Haug, H. (1977). Experimental approaches for exciton Bose-Einstein condensation. *Phys. Rep., Phys. Lett.,* Vol.33, pp. 209

Hasselbeck, M. P.; Stalnaker, D.L.; Schlie, A.; Rotter, T. J.; Stintz, A. & Sheik-Bahae, M. (2002). Emission of terahertz radiation from coupled plasmon-phonon modes in InAs. *Phys. Rev. B* Vol.65, 233203

Haug, H. & Koch, S.W. (2009). *Quantum Theory of the Optical and Electronic Properties of Semiconductors*, 5th ed., World Scientific, Singapore

Haug, H & Jauho, A.P. (1996). *Quantum Kinetics in Transport and Optics of Semiconductors*, Springer, Berlin.

Hirtschulz, M.; Milde, F.; Malić, E.; Butscher, S.; Thomsen, C.; Reich, S.; & Knorr, A. (2008). Carbon nanotube Bloch equations: A many-body approach to nonlinear and ultrafast optical properties. *Phys. Rev. B*, Vol.77, 035403

Huber, R.; Kaindl, R.A.; Schmid, B.A & Chemla, D.S. (2005a). Broadband terahertz study of excitonic resonances in the high-density regime in GaAs/$Al_xGa_{1-x}As$ quantum wells. *Phys. Rev. B*, Vol.72, 161314(R)

Huber, R.; Kubler, C.; Tubel, S.; Leitenstorfer, A.; Vu, Q. T.; Haug, H.; Kohler F. & Amann, M.C. (2005b). Femtosecond Formation of Coupled Phonon-Plasmon Modes in InP: Ultrabroadband THz Experiment and Quantum Kinetic Theory, *Phys. Rev. Lett.*, Vol.94, 027401

Kaindl, R. A.; Hagele, D.; Carnahan, M. A. & Chemla, D.S. (2009). Transient terahertz spectroscopy of excitons and unbound carriers in quasi-two-dimensional electron-hole gases. *Phys. Rev. B*, Vol. 79, 045320

Kapetanakis, M. D.; Perakis, I. E.; Wickey, K. J.; Piermarocchi, C. & Wang, J. (2009). Femtosecond Coherent Control of Spins in (Ga,Mn)As Ferromagnetic Semiconductors using Light. *Phys. Rev. Lett.*, Vol.103, 047404

Kersting, R.; Unterrainer, K.; Strasser, G.; Kauffmann, H. & Gornik, E. (1997). Few-Cycle THz Emission from Cold Plasma Oscillations. *Phys. Rev. Lett.*, Vol.79, pp. 3038

Kira, M.; Jahnke, F.; Hoyer, W. & Koch, S.W. (1999). Quantum theory of spontaneous emission and coherent effects in semiconductor microstructures. *Progress in Quantum Electronics*, Vol.23, pp. 189

Kono, S.; Tani, M.; Gu, P. & Sakai, K. (2000). Detection of up to 20 THz with a low-Temperature-grown GaAs Antenna gated with 15 fs Light Pulses. *Appl. Phys. Lett.*, Vol.77, pp. 4104

Krauß, M.; Aeschlimann, M. & Schneider, H.C. (2008). Ultrafast Spin Dynamics Including Spin-Orbit Interaction in Semiconductors, *Phys. Rev. Lett.*, Vol.100, 256601

Leitenstorfer, A.; Hunsche, S.; Shah, J.; Nuss, M.C.; & Knox, W.H. (1999). Detectors and Sources for Ultrabroadband Electro-optic Sampling: Experiment and Theory. *Appl. Phys. Lett.*, Vol.74, pp. 1516

Lindberg, M. & Koch, S.W. (1988). Effective Bloch equations for Semiconductors. *Phys. Rev. B,* Vol.38, No.5, pp. 3342

Lopez-Sancho, M.P.; Muñoz, M.C. & Chico, L. (2001). Coulomb Interactions in Carbon Nanotubes. *Phys. Rev. B*, Vol.63, 165419

Ma, J. & Yuan, R.K. (1998). Electronic and Optical Properties of finite zigzag Carbon Nanotubes with and without Coulomb Interaction. *Phys. Rev. B*, Vol.57, pp. 9343

Mahan, G.D. (2007). *Many Particle Physics* 3rd ed, Springer

Makhonin, M.N.; Chekhovich, E.A.; Senellart, P.; Lemaître, A.; Skolnick, M.S. & Tartakovskii, A.I. (2010). Optically tunable Nuclear Magnetic Resonance in a single Quantum Dot. *Phys. Rev. B*, Vol.82, 161309(R)

Meier, T.; Reichelt, M.; Koch, S.W. & Höfer, U. (2005) Femtosecond time-resolved five-wave mixing at silicon surfaces, *J.Phys. Condens. Matter, Vol.*17, S221

Mooradian, A. & Wright, G.B. (1966). Observation of the Interaction of Plasmons with Longitudinal Optical Phonons in GaAs. *Phys. Rev. Lett.*, Vol.16, pp. 999

Nagai, M.; Shimano, R. & Kuwata-Gonokami, M. (2001). Electron-Hole Droplet Formation in Direct-Gap Semiconductors Observed by Mid-Infrared Pump-Probe Spectroscopy. *Phys. Rev. Lett.*, Vol. 86, pp.5795

Ogawa, T.; Tomio, Y. & Asano, K. (2007). Quantum Condensation in Electron-hole Systems: Excitonic BEC-BCS Crossover and Biexciton Crystallisation. *J. Phys. Condens. Matter*, Vol.19, 295205.

Perebeinos, V. ; Tersoff, J. & Avouris, P. (2004). Scaling of Excitons in Carbon Nanotubes. *Phys. Rev. Lett.*, Vol.92, 257402

Proietti Zaccaria, R. & Rossi. F. (2003). On the problem of generalizing the Semiconductor Bloch equation from a closed to an open System. *Phys. Rev. B, Vol.67*, 113311

Ridley, B.K. (2000). *Quantum Processes in Semiconductors*, Qxford

Rossi, F. & Kuhn, T. (2002). Theory of Ultrafast Phenomena in Photoexcited Semiconductors. *Rev. Mod. Phys.*, Vol.74, pp. 895

Rossi, F.; Di Carlo, A & Lugli, P. (1998). Microscopic Theory of Quantum-Transport Phenomena in Mesoscopic Systems: A Monte Carlo Approach. *Phys. Rev. Lett., Vol.80*, pp. 3348

Rössler, U; Tejedor, C. & Vina, L. (2003). Semiconductor Bloch Equations including Spin and Polarization Degrees of Freedom, in *Physics of Semiconductors 2002. Institute of Physics Conference Serie*s 171, A.R. Long & J.H. Davies, (Eds.), IOP Publishing Bristol, UK

Sandhu, J.S; Heberle, A.P.; Baumberg, J.J. & Cleaver, J.R.A. (2001). Gateable Suppression of Spin Relaxation in Semiconductors. *Phys. Rev. Lett.*, Vol.86, pp. 2150

Shah, J. (1999). *Ultrafast Spectroscopy of Semiconductors and Semiconductor Nanostructures*, Springer

Spataru, J.R.A; Ismail-Beigi, S; Benedict, L.X & Louie, S.G. (2004). Excitonic Effects and Optical Spectra of Single-Walled Carbon Nanotubes. *Phys. Rev. Lett., Vol.92,* 077402

Storebo, A.K; Brudevoll, T. & Stenersen, K. (2010). Numerical Modeling of IR-Laser-Irradiated HgCdTe. *Journal of Electronic Materials*, Vol.39, No.10, pp. 2220

Suzuki, T. & Shimano R. (2011). Cooling Dynamics of photoexcited Carriers in Si studied using optical Pump and terahertz Probe Spectroscopy. *Phys. Rev. B*, Vol.83, 085207

Voelkmann, C.; Reichelt, M.; Meier, T.; Koch, S.W. & Höfer, U. (2004). Five-Wave-Mixing Spectroscopy of Ultrafast Electron Dynamics at a Si(001) Surface, *Phys. Rev. Lett.*, Vol.92, 127405

Vu, Q.T. & Haug, H. (2000). Time-dependent Screening of the Carrier-Phonon and Carrier-Carrier Interactions in nonequilibrium Systems. *Phys Rev. B,* Vol.62, pp. 7179

Wang, D. & Dignam, M.M. (2009). Excitonic Approach to the ultrafast Optical Response of Semiconductor Quantum Wells. *Phys Rev.B,* Vol.79, 165320

Wang, D. (2008). Ph.D. thesis. Queen's University, 2008. Available at URL: http://hdl.handle.net/1974/1593.

Wang, W.; Zhang, J. & Lenstra, D. (2006). Semiconductor Optical Bloch Equations explain polarization dependent FourWave Mixing Quantum Beats in bulk Semiconductors. *Proceedings, Symposium IEEE/LEOS Benelux Chapter*, pp. 249, Eindhoven (2006)

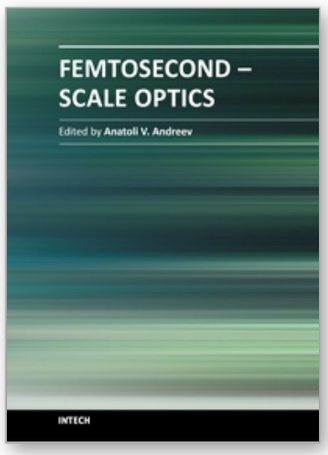

Femtosecond-Scale Optics
Edited by Prof. Anatoly Andreev

ISBN 978-953-307-769-7
Hard cover, 434 pages
Publisher InTech
Published online 14, November, 2011
Published in print edition November, 2011

With progress in ultrashort ultraintense laser technologies the peak power of a laser pulse increases year by year. These new instruments accessible to a large community of researchers revolutionized experiments in nonlinear optics because when laser pulse intensity exceeds or even approaches intra-atomic field strength the new physical picture of light-matter interaction appears. Laser radiation is efficiently transformed into fluxes of charged or neutral particles and the very wide band of electromagnetic emission (from THz up to x-rays) is observed. The traditional phenomena of nonlinear optics as harmonic generation, self-focusing, ionization, etc, demonstrate the drastically different dependency on the laser pulse intensity in contrast the well known rules. This field of researches is in rapid progress now. The presented papers provide a description of recent developments and original results obtained by authors in some specific areas of this very wide scientific field. We hope that the Volume will be of interest for those specialized in the subject of laser-matter interactions.

How to reference
In order to correctly reference this scholarly work, feel free to copy and paste the following:

T. Brudevoll, A. K. Storebo, O. Skaaring, C. N. Kirkemo, O. C. Norum, O. Olsen and M. Breivik (2011). Time-Resolved Laser Spectroscopy of Semiconductors - Physical Processes and Methods of Analysis, Femtosecond-Scale Optics, Prof. Anatoly Andreev (Ed.), ISBN: 978-953-307-769-7, InTech, Available from: http://www.intechopen.com/books/femtosecond-scale-optics/time-resolved-laser-spectroscopy-of-semiconductors-physical-processes-and-methods-of-analysis

INTECH
open science | open minds

InTech Europe
University Campus STeP Ri
Slavka Krautzeka 83/A
51000 Rijeka, Croatia
Phone: +385 (51) 770 447
Fax: +385 (51) 686 166
www.intechopen.com

InTech China
Unit 405, Office Block, Hotel Equatorial Shanghai
No.65, Yan An Road (West), Shanghai, 200040, China
中国上海市延安西路65号上海国际贵都大饭店办公楼405单元
Phone: +86-21-62489820
Fax: +86-21-62489821

IntechOpen